

OPEN ACCESS

**Repository of the Max Delbrück Center for Molecular Medicine (MDC)
in the Helmholtz Association**

<https://edoc.mdc-berlin.de/15946>

Natural killer cell reduction and uteroplacental vasculopathy

Golic, M., Haase, N., Herse, F., Wehner, A., Vercruysse, L., Pijnenborg, R., Balogh, A., Saether, P.C., Dissen, E., Luft, F.C., Przybyl, L., Park, J.K., Alnaes-Katjavivi, P., Staff, A.C., Verlohren, S., Henrich, W., Muller, D.N., Dechend, R.

This is a copy of the accepted manuscript, as originally published online ahead of print by the American Heart Association. The original article has been published in final edited form in:

Hypertension
2016 OCT ; 68(4): 964-973
2016 AUG 22 (first published online: final publication)
doi: [10.1161/HYPERTENSIONAHA.116.07800](https://doi.org/10.1161/HYPERTENSIONAHA.116.07800)

Publisher: [American Heart Association | Lippincott Williams & Wilkins](#)

© 2016 American Heart Association, Inc.

Natural Killer Cell Reduction and Uteroplacental Vasculopathy

Michaela Golic, Nadine Haase, Florian Herse, Anika Wehner, Lisbeth Vercruyse, Robert Pijnenborg, Andras Balogh, Per Christian Saether, Erik Dissen, Friedrich C. Luft, Lukasz Przybyl, Joon-Keun Park, Patji Alnaes-Katjavivi, Anne Cathrine Staff, Stefan Verlohren, Wolfgang Henrich, Dominik N. Muller, Ralf Dechend

Abstract—Uterine natural killer cells are important for uteroplacental development and pregnancy maintenance. Their role in pregnancy disorders, such as preeclampsia, is unknown. We reduced the number of natural killer cells by administering rabbit anti-asialo GM1 antiserum in an established rat preeclamptic model (female human angiotensinogen×male human renin) and evaluated the effects at the end of pregnancy (day 21), compared with preeclamptic control rats receiving normal rabbit serum. In 100% of the antiserum-treated, preeclamptic rats (7/7), we observed highly degenerated vessel cross sections in the mesometrial triangle at the end of pregnancy. This maternal uterine vasculopathy was characterized by a total absence of nucleated/living cells in the vessel wall and perivascularly and prominent presence of fibrosis. Furthermore, there were no endovascular trophoblast cells within the vessel lumen. In the control, normal rabbit serum-treated, preeclamptic rats, only 20% (1/5) of the animals displayed such vasculopathy. We confirmed the results in healthy pregnant wild-type rats: after anti-asialo GM1 treatment, 67% of maternal rats displayed vasculopathy at the end of pregnancy compared with 0% in rabbit serum-treated control rats. This vasculopathy was associated with a significantly lower fetal weight in wild-type rats and deterioration of fetal brain/liver weight ratio in preeclamptic rats. Anti-asialo GM1 application had no influence on maternal hypertension and albuminuria during pregnancy. Our results show a new role of natural killer cells during hypertensive pregnancy in maintaining vascular integrity. In normotensive pregnancy, this integrity seems important for fetal growth. (*Hypertension*. 2016;68:00-00. DOI: 10.1161/HYPERTENSIONAHA.116.07800.) • [Online Data Supplement](#)

Key Words: angiotensinogen ■ immunity ■ natural killer cells ■ preeclampsia ■ rat

Humans, high-order primates, and rodents display hemochorial placentation characterized by direct contact of maternal blood with fetal chorionic trophoblast cells to optimize fetal-maternal interactions.¹⁻³ Hemochorial placentation requires trophoblast cell invasion into uterine tissue, which is associated with remodeling of uterine spiral arteries.⁴ Both trophoblast cell invasion and spiral artery remodeling are key steps to allow optimal gas exchange and nutrient supply to the developing fetus. In the human, failure of these processes may result in intrauterine growth restriction and preeclampsia.⁵ Preeclampsia is a multisystemic pregnancy disorder,

featuring new-onset maternal hypertension and proteinuria after 20 weeks of gestation.⁶ In many cases, preeclampsia is associated with a growth-restricted fetus.⁷ Preeclampsia is also associated with long-term, increased, cardiovascular risk for both mother⁸ and child.⁹ Recently, circulating antiangiogenic factors¹⁰ and unappreciated maternal immune recognition of the fetus¹¹ have shed mechanistic light on preeclampsia. The invasion of the semiallogenic zygote-derived trophoblast cells into the maternal uterus requires a tolerant maternal immune milieu. Failed tolerance could explain the typical, shallow, trophoblast cell invasion in preeclampsia. Uterine natural killer

Received May 3, 2016; first decision May 23, 2016; revision accepted July 31, 2016.

From the Experimental and Clinical Research Center, a cooperation between the Max Delbrück Center for Molecular Medicine in the Helmholtz Association and the Charité - Universitätsmedizin Berlin, Germany (M.G., N.H., F.H., A.W., A.B., F.C.L., L.P., D.N.M., R.D.); Department of Obstetrics (M.G., S.V., W.H.) and Department of Gynecology (M.G.), Charité - Universitätsmedizin Berlin, Germany; Berlin Institute of Health (BIH), Germany (M.G., N.H., F.H., A.W., A.B., F.C.L., L.P., S.V., D.N.M., R.D.); Max Delbrück Center for Molecular Medicine in the Helmholtz Association, Berlin, Germany (N.H., F.H., A.B., D.N.M.); Charité - Universitätsmedizin Berlin, Campus Berlin Buch, Germany (A.W., F.C.L., L.P., R.D.); Department of Development and Regeneration, University Hospital Leuven, Belgium (L.V., R.P.); Department of Medical Biology, János Szentágotthai Research Centre Pécs, University of Pécs Medical School, Hungary (A.B.); Department of Molecular Medicine, Institute of Basic Medical Sciences, University of Oslo, Norway (P.C.S., E.D.); Department of Multi-Disciplinary Laboratory Medicine and Medical Biochemistry, Akershus University Hospital, Lørenskog, Norway (P.C.S.); Clinic for Nephrology and Hypertension, Hannover Medical School, Germany (J.-K.P.); University of Oslo, Norway (P.A.-K., A.C.S.); Department of Obstetrics and Gynecology, Oslo University Hospital, Norway (P.A.-K., A.C.S.); and Department of Cardiology and Nephrology, HELIOS Klinikum Berlin, Germany (R.D.).

The online-only Data Supplement is available with this article at <http://hyper.ahajournals.org/lookup/suppl/doi:10.1161/HYPERTENSIONAHA.116.07800/-/DC1>.

Correspondence to Ralf Dechend, Experimental and Clinical Research Center, Lindenberger Weg 80, 13125 Berlin, Germany. E-mail ralf.dechend@charite.de

© 2016 American Heart Association, Inc.

Hypertension is available at <http://hyper.ahajournals.org>

DOI: 10.1161/HYPERTENSIONAHA.116.07800

(uNK) cells make up the majority of leucocytes in the uterine implantation site.¹² Although uNK cells contain perforin and granzyme-filled cytoplasmic granules, they exhibit less cytotoxic activity against major histocompatibility complex class-I-negative target cells, compared with circulating natural killer (NK) cells.¹³ Furthermore, uNK cells do not exhibit NK activity against trophoblast cells.¹⁴ In the decidua of preeclamptic patients, changes in uNK cells and T-lymphocyte subsets could affect local immunoregulatory mechanisms.¹⁵

Chakraborty et al¹⁶ showed that in rats, uNK cells are involved in hemochorial placentation by regulating trophoblast cell lineage decisions. Moreover, they presented results showing that endovascular trophoblast cell invasion is increased in wild-type rats during midpregnancy after depletion of uNK cells. However, they did not examine effects on late and pathological pregnancies. Because shallow endovascular trophoblast cell invasion is considered to be causal for the pathological event initiating preeclampsia symptoms and signs,¹⁷ we hypothesized that depletion or reduction of NK cells associated with increased trophoblast cell invasion ameliorates the preeclamptic phenotype in our rat model. We worked with our double-transgenic rat preeclamptic model where the preeclamptic phenotype has been established in rats¹⁸ and mice.¹⁹ The dams expressing human angiotensinogen develop hypertension and proteinuria during pregnancy after mating with males expressing the human renin.¹⁸ The offspring are growth restricted,²⁰ comparable to what is observed in spontaneously occurring, early-onset preeclampsia in pregnant women. The model exhibits pathological endovascular trophoblast cell invasion with altered uteroplacental vascular remodeling.^{21,22}

Methods

Local government authorities approved the studies along guidelines provided by the American Physiological Society. Detailed description of methods is available in the [online-only Data Supplement](#).

Analysis of Maternal Uterine Vasculopathy

One uteroplacental unit per mother rat was investigated for analysis of maternal vasculopathy (n=7 anti-asialo GM1-treated, preeclamptic rats versus n=5 normal rabbit serum-treated, control, preeclamptic rats, and n=6 anti-asialo GM1-treated, wild-type, Sprague-Dawley [SD] rats versus n=5 normal rabbit serum-treated, SD control rats). In preeclamptic rats, at least 4 series of sections from the center of the uteroplacental unit were examined per rat. Each series consisted of 10 consecutive sections, 3 μ m thick. The distance between the series was 100 μ m. In SD rats, at least 15 series of sections from the uteroplacental unit were examined (also covering the central parts). Each series consisted of at least 5 consecutive sections, 3 μ m thick. The distance within the series was 100 μ m. Terminal deoxynucleotidyl transferase dUTP nick end labeling assay was performed with the TMR In Situ Cell Death Detection Kit (Roche) as recommended by the manufacturer. To visualize cell nuclei, slides were counterstained with the DNA dye Hoechst 33342 (Sigma) and mounted using Vectashield antifade mounting medium (Vector Laboratories). Sections were investigated and imaged by Zeiss Axio Imager M2 fluorescence upright microscope (Zeiss) using either \times 10 or \times 40 Plan-Apochromat objectives (Zeiss). Pictures were taken with the AxioCam HRc camera (Zeiss).

Statistics

All statistics were done with GraphPad Prism 6. The blood pressure data were analyzed by repeated-measures 2-way ANOVA and

Bonferroni multiple comparisons test. With all other data, Grubb test was performed, outliers were excluded (exception: resorption data), and normal distribution calculated by Kolmogorov–Smirnov test or D'Agostino–Pearson omnibus normality test. For group differences, either the unpaired *t* test (for normally distributed data) or the Mann–Whitney test (for not normally distributed data) was applied. In case of different variances within normally distributed data, an unpaired *t* test with Welch correction was performed. The quantitative, real-time, reverse transcription polymerase chain reaction results on mesometrial triangle with regard to uNK cells were evaluated with the nonparametric 1-way ANOVA, Kruskal–Wallis test, and Dunn multiple comparisons test. Values are shown as mean \pm SEM (normally distributed data) or median with interquartile range (not normally distributed data). *P* values <0.05 were considered significant (*), *P*<0.01 (**), *P*<0.001 (***), and *P*<0.0001 (****).

Results

Reduction of Uterine Natural Killer Cells in Preeclamptic Rats on Pregnancy Day 15 After Anti-Asialo GM1 Application

We first investigated whether NK cell reduction on pregnancy day 15 was successful after anti-asialo GM1 therapy in preeclamptic rats. In control, rabbit serum-treated, preeclamptic dams on day 15 of pregnancy, 2.5 \pm 0.1% of the splenic lymphocytes were NK cells (CD161 positive and CD3 negative), whereas only 0.5 \pm 0.0% of the splenic lymphocytes were NK cells after anti-asialo GM1 treatment, which means that the NK cell population was reduced by 80% (Figure 1A). In the mesometrial triangle of the uteroplacental unit of preeclamptic rats, NK cells were also decreased after anti-asialo GM1 therapy (Figure 1B through 1D). Immunohistochemical analysis on day 15 of pregnancy demonstrated that uNK cells were present around vessels in control, rabbit serum-treated, preeclamptic rats (Figure 1B, left) but were significantly reduced after anti-asialo GM1 administration (Figure 1B, right). Quantification revealed that anti-asialo GM1 treatment reduced the number of uNK cells in the mesometrial triangle of preeclamptic rats by 60% (Figure 1C). This finding was confirmed by quantitative, real-time, reverse transcription polymerase chain reaction (Figure 1D) in the uteroplacental unit of preeclamptic rats on pregnancy day 15, showing that the mRNA expression of the NK cell marker Nkp46 (natural cytotoxicity receptor 1), expressed by all rat conventional NK cells, was decreased by 89%. As expected, uNK cells were hardly present in the uteroplacental unit of preeclamptic rats at the end of pregnancy (day 21), irrespective of anti-asialo GM1 treatment.

Maternal Vasculopathy in the Uterus of Preeclamptic Rats on Pregnancy Day 21 After Anti-Asialo GM1 Application

After anti-asialo GM1 application, we found degenerative spiral artery cross sections surrounded by cell detritus and fibrosis in the mesometrial triangle of preeclamptic rats, the maternal part of the uteroplacental unit (Figure 2A through 2E; Figure S1A through S1E in the [online-only Data Supplement](#)). We observed in every anti-asialo GM1-treated, preeclamptic mother rat (7/7, 100%) at least one of such pathological cross section at the end of pregnancy (Figure

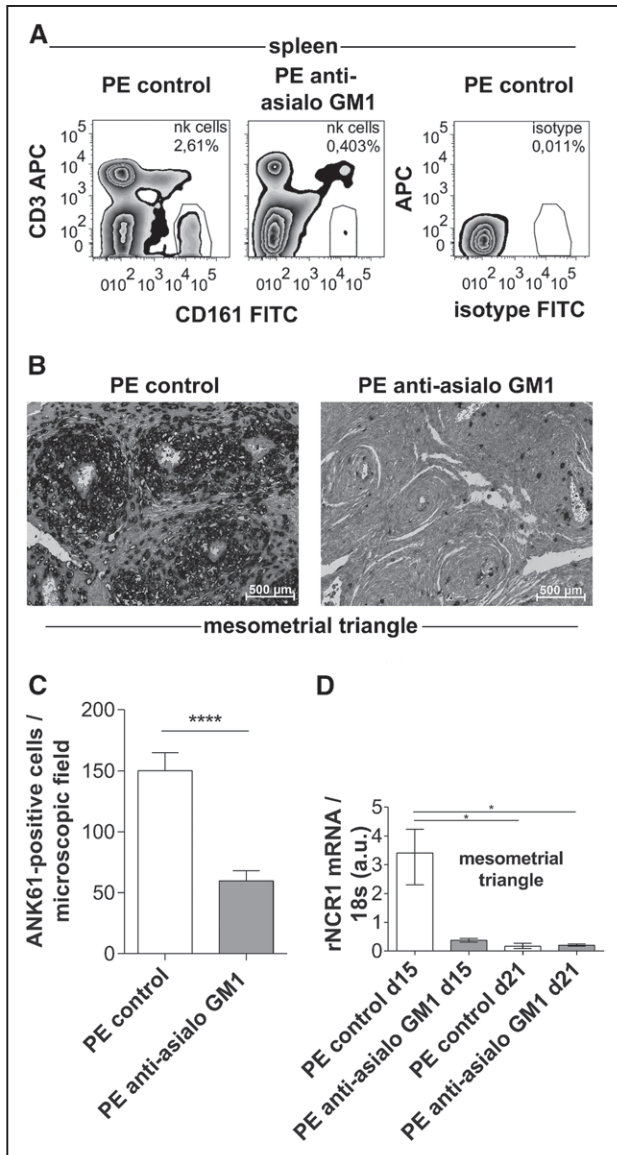


Figure 1. Reduction of natural killer cells on pregnancy day 15 in preeclamptic (PE) rats. **A**, Anti-asialo GM1 reduced natural killer cells (NK cells) in the maternal spleen of PE rats on pregnancy day 15 by 80% ($n=3$ per group). Two-color, flow cytometry contour plots displaying CD161 fluorescein isothiocyanate (FITC) vs CD3 allophycocyanin (APC), or isotype control. **B**, Histological section images from the mesometrial triangle on day 15 of pregnancy of a control, rabbit serum-treated and an anti-asialo GM1-treated PE rat, respectively, $\times 20$ magnification. Immunohistochemical staining with anti-natural killer cell activation structures (ANK61) to detect uterine natural killer cells (uNK cells), which appear in black after nitro-blue tetrazolium chloride and 5-bromo-4-chloro-3'-indolylphosphate p-toluidine salt staining and counterstaining with periodic acid-Schiff and hematoxylin. Anti-asialo GM1 reduced uNK cells in the mesometrial triangle of PE rats on pregnancy day 15. **C**, Quantification of the ANK61-positive staining of mesometrial triangles of PE rats on pregnancy day 15. Positive cells were evaluated semiquantitatively by counting them in 3 complete microscopic fields per mesometrial triangle ($n=3$ mesometrial triangles from anti-asialo GM1-treated PE rats and $n=3$ mesometrial triangles from control rabbit serum-treated PE rats, all mesometrial triangles from different mother rats). Anti-asialo GM1 reduced the mean number of ANK-positive cells in the mesometrial triangle by 60% (60 ± 8 cells per microscopic field in $\times 40$ magnification vs 150 ± 15 cells in the PE, control, rabbit serum-treated group; $P < 0.0001$, unpaired t test, (Continued)

characterized by the absence of cell nuclear staining in perivascular cells and in the vascular smooth muscle cells of the vessel wall (Figure 3B). Vascular smooth muscle cells were not detectable in these cross sections (Figure 2C), and endovascular trophoblast cells were almost totally absent (Figure 2D). Moreover, there was increased presence of apoptotic cells within the vasculopathy (Figure 3B).

Trophoblast Cell Invasion in Preeclamptic Rats on Pregnancy Day 21 After Anti-asialo GM1 Application

After anti-asialo GM1 application, interstitial trophoblast cell invasion (Figure S2A) into the mesometrial triangle of preeclamptic rats was diminished at the end of pregnancy (gestational day 21). In parallel, the number of trophoblast cells in the successfully invaded mesometrial triangle was significantly decreased after anti-asialo GM1 (Figure S2B).

Endovascular trophoblast cell invasion into the mesometrial triangle of preeclamptic rats (Figure S3A through S3C) was unchanged after anti-asialo GM1 treatment. This finding corresponded to the unchanged amount of vascular smooth muscle α -actin in trophoblast cell-invaded arteries (Figure S3D and S3E), indicating an unchanged spiral artery remodeling. The number of spiral artery cross sections in the mesometrial triangle of preeclamptic rats was not different after anti-asialo GM1 treatment (data not shown).

Angiogenic Factors and Interleukin 15 in Uteroplacental Unit of Preeclamptic Rats on Pregnancy Day 21 After Anti-Asialo GM1 Application

We further investigated the uteroplacental units of preeclamptic rats on pregnancy day 21. In the placenta, the fetal part of the uteroplacental unit, anti-asialo GM1 application decreased soluble, fms-like tyrosine kinase 1 (sFLT-1; Figure S4A) and placental growth factor (PlGF; Figure S4B) protein concentration, leading to an unchanged sFLT-1/PlGF ratio in preeclamptic rats (Figure S4C). Gene expression of sFLT-1 and PlGF in placenta was not different between the 2 preeclamptic groups (data not shown). In mesometrial triangle of preeclamptic rats, the maternal part of the uteroplacental unit, there was neither

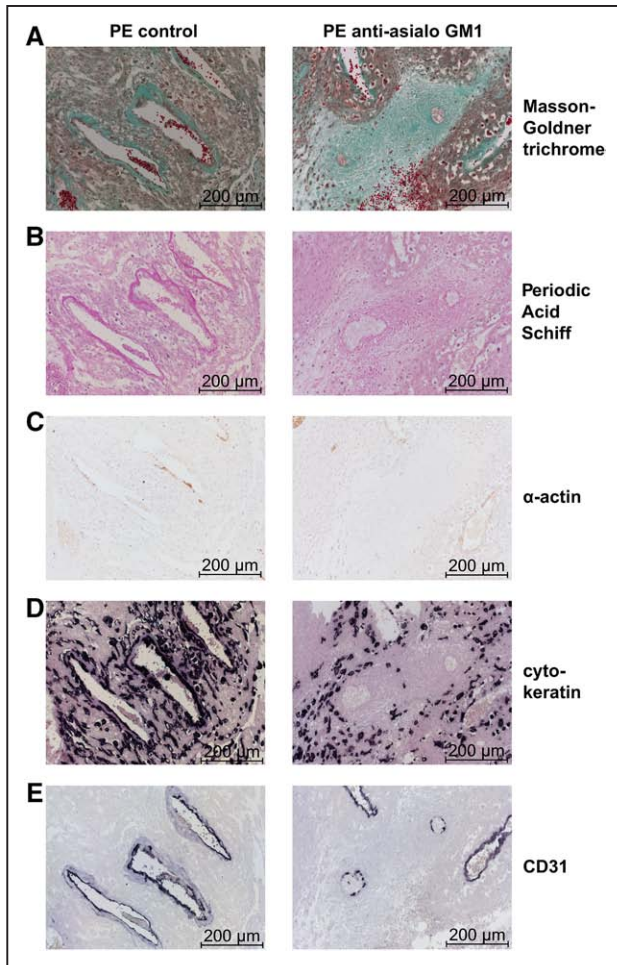


Figure 2. Influence of anti-asialo GM1 on maternal uterine vessels in preeclamptic (PE) rats on pregnancy day 21. Photomicrographs of degenerative maternal vasculopathy in the mesometrial triangle of PE rats. In every anti-asialo GM1-treated, PE rat ($n=7$), we found at least one degenerative vessel cross section with massive fibrosis. In control, rabbit serum-treated PE rats ($n=5$), just one mother rat displayed vasculopathy. Shown are representative parallel stainings of an anti-asialo GM1-treated, PE rat and a control, rabbit serum-treated PE rat. **A**, Masson–Goldner trichrome staining, which typically stains collagen green. Around the vessels in the anti-asialo GM1-treated, PE rat, there is a huge perivascular collagen accumulation/fibrosis, which is not present in the control, rabbit serum-treated PE mesometrial triangle. The lumen of the spiral artery in the anti-asialo GM1-treated, PE rat seems almost totally filled with cells and exudate with just a minority being erythrocytes (red in Masson–Goldner trichrome staining). **B**, Periodic acid–Schiff (PAS) staining and counterstaining with hematoxylin. In the anti-asialo GM1-treated, PE rat, there are a lot of rounded cells, which have lost their connectivity. These cells show no nuclear staining with hematoxylin, indicating an advanced cell damage. **C**, Diaminobenzidine staining of α -actin and counterstaining with PAS and hematoxylin, after which smooth muscle cells usually appear in brown. In the wall of degenerative vessels (in the anti-asialo GM1-treated, PE rat), there was no α -actin of smooth muscle cells detectable anymore. **D**, Cytokeratin staining of trophoblast cells, which appear in black after nitro-blue tetrazolium chloride (NBT) and 5-bromo-4-chloro-3'-indolylphosphate p-toluidine salt (BCIP) staining and counterstaining with PAS and hematoxylin. The degenerative vessel cross sections in the anti-asialo GM1-treated PE rat are hardly infiltrated by endovascular trophoblast cells, whereas there are a lot of interstitial trophoblast cells present. **E**, CD31 staining of endothelial cells (NBT and BCIP staining and (Continued)

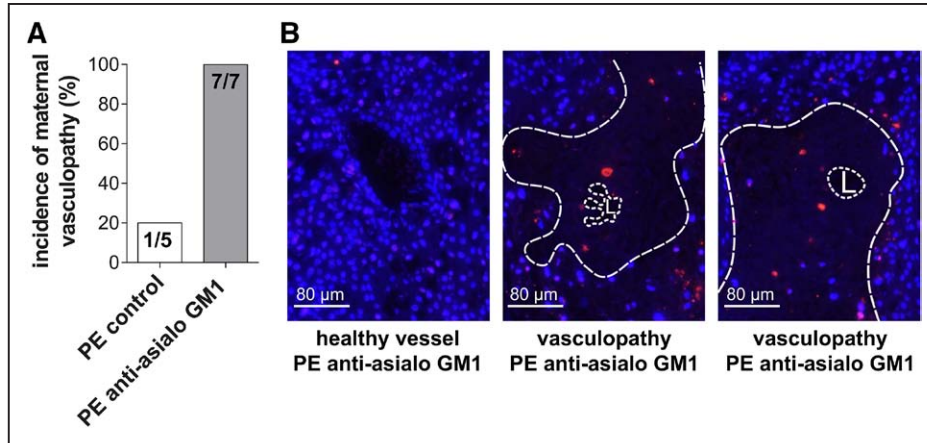
a difference in protein concentration of sFLT-1 (Figure S4A) and PIGF (Figure S4B), nor in the ratio of both (Figure S4C). Gene expression displayed similar results (data not shown). The sFLT-1/PLGF ratio in maternal preeclamptic plasma at the end of pregnancy was also unchanged (Figure S4D). Anti-asialo GM1 decreased gene expression of interleukin 15 in the preeclamptic placenta by 14% (Figure S4E) and increased it in the mesometrial triangle by 47%.

Influence of Anti-Asialo GM1 Application on Fetal Outcome and Maternal Phenotype in Preeclamptic Rats on Pregnancy Day 21

We then analyzed the influence of anti-asialo GM1 treatment on fetuses of preeclamptic rats, concentrating on intrauterine growth retardation on pregnancy day 21. Anti-asialo GM1 application increased fetal brain/liver weight ratio in preeclamptic rats (Figure 4A). Fetal liver weight (Figure S5A) was decreased, whereas fetal brain weight (Figure S5B) and total fetal weight (Figure 4B) in preeclamptic rats remained unchanged. There was neither a difference in the number of fetuses (Figure S5C), nor in the number of resorptions per mother rat (Figure S5D) between the 2 preeclamptic groups. In preeclamptic mother rats, NK cell reduction did not influence the preeclampsia-defining signs, hypertension (Figure 4C) and albuminuria (Figure S5E). Systolic and diastolic blood pressure measured by telemetry showed no difference between both preeclamptic groups (data not shown). Additionally, serum creatinine (Figure S5F), serum cystatin C (Figure S5G), and maternal body weight (Figure S5H) were not changed in preeclamptic rats after anti-asialo GM1 application. The uteroplacental units (Figure 4D) were heavier, and the uteroplacental unit/fetal weight ratio (Figure 4E) was increased in preeclamptic rats after anti-asialo GM1 application.

Influence of Anti-Asialo GM1 Application in Wild-Type Rats on Pregnancy Day 21

We finally investigated the influence of anti-asialo GM1 application on healthy, wild-type, SD rats on pregnancy day 21. Anti-asialo GM1 or rabbit serum, respectively, was applied according to the same protocol used in our preeclamptic rats. We found uterine maternal vasculopathy in 66.7% (4/6) of anti-asialo GM1-treated, SD mother rats (Figure 5A). None of the rabbit serum-treated, control SD mothers displayed uterine vasculopathy. One anti-asialo GM1-treated, SD mother rat carried 11 implantation sites with 10 resorptions and 1 highly growth-restricted fetus (1.6 g). In the center of this specimen's mesometrial triangle (Figure 5B), there was a large area completely lacking nuclear staining. Within this area, we discovered several vessel cross sections displaying vasculopathy and increased terminal deoxynucleotidyl transferase dUTP nick end labeling positivity. In SD rats, anti-asialo GM1 decreased fetal weight significantly (3.7 versus 3.9 g in the control rabbit



serum SD group; Figure 5C). Fetal brain/liver weight ratio (Figure 5D; Figure S6A and S6B), weight of uteroplacental unit (Figure 5E), and the uteroplacental unit/fetal weight ratio (Figure 5F) were unchanged between both SD groups. Moreover, maternal blood pressure, albuminuria, and number of fetuses and resorptions were not changed after anti-asialo GM1 treatment in SD rats in comparison to rabbit serum-treated SD rats (data not shown).

Discussion

We successfully reduced NK cell numbers in our preeclamptic rats by administering anti-asialo GM1 antiserum. This effect was associated with a pathological phenotype at the fetal–maternal interface. Maternal uterine vasculopathy with presumably dead cells in the vessel wall and in the perivascular zone occurred in every preeclamptic and in the majority of wild-type SD rats after anti-asialo GM1 application. The vasculopathy was associated with a deterioration of fetal outcome, which was more pronounced in SD rats where fetal weight was reduced. Fetuses of preeclamptic rats displayed signs of growth restriction (increased fetal brain/liver weight ratio as a marker for fetal centralization) after anti-asialo therapy. Reduction of NK cells by anti-asialo GM1 administration diminished the area and the density of interstitial trophoblast cell invasion in preeclamptic rats. There was no change in blood pressure and albuminuria neither in preeclamptic nor in SD rats after anti-asialo GM1 treatment.

A vasculopathy associated with NK cell reduction in hypertensive pregnancy has heretofore never been shown. These data agree with seminal earlier work showing that absent NK cells during normotensive murine pregnancy is associated with uterine vasculopathy suggestive of arteriosclerosis and fetal loss.²³ Moreover, others have demonstrated involvement of uNK cells in decidual angiogenesis that supports fetal growth during early and mid pregnancy.²⁴ We observed degenerated maternal vessels with massive dead tissue and fibrosis

in the mesometrial triangle of NK-reduced animals. We are aware that identifying vascular smooth muscle cell degeneration is difficult and that absent nuclear staining in perivascular cells as signs of an expanding degeneration of the surrounding tissue is imprecise. We interpret our result a nonspecific degenerative process, involving also the perivascular area. Isolated round cells with a loss of connectivity were occasionally observed in other mesometrial triangles, either anti-asialo GM1-treated or in control rabbit serum-treated rats; however, on a much smaller scale.

Our findings could also suggest that NK cells are involved in maintenance and protection of the maternal uterine vascular system, perhaps even with long-term implications. The vasculopathy was associated with fetal growth restriction in wild-type SD rats, and subtle signs of fetal growth restriction effects were observed in preeclamptic rats, even though these fetuses were already extremely growth restricted (>20% growth restriction in comparison to healthy wild-type SD fetuses). We hypothesize that the vasculopathy arose during the last third of pregnancy because we did not observe vasculopathy in mesometrial triangles of preeclamptic rats on pregnancy day 15 (data not shown). We regard the vasculopathy as representing final exhaustion at the end of pregnancy when the stress exerted on the maternal cardiovascular system increases significantly. In addition, the degenerated vessels with absence of intraluminal cells could explain why we could not reproduce the results reported by Chakraborty et al.¹⁶ They reported increased endovascular trophoblast cell invasion on pregnancy day 14 in wild-type rats after anti-asialo GM1 administration. In our study of preeclamptic rats on pregnancy day 21, endovascular trophoblast cell invasion was not different from controls. Besides vasculopathy, this conflicting result could also be because of the different time points of analysis and the fact that Chakraborty et al used healthy wild-type rats, whereas we tested NK cell reduction in a transgenic preeclamptic model. Chakraborty et al did

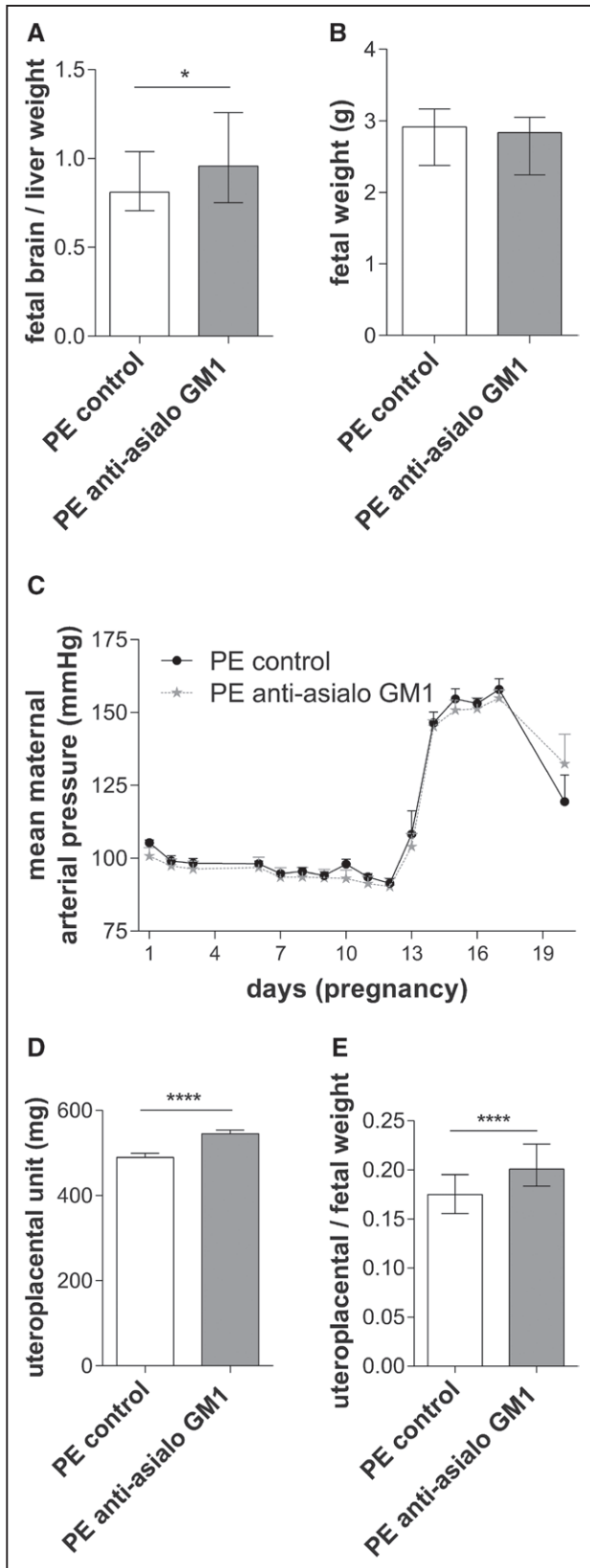


Figure 4. Influence of anti-asialo GM1 on fetal outcome and maternal blood pressure in preeclamptic (PE) rats on pregnancy day 21. **A**, Anti-asialo GM1 increased fetal brain/liver weight ratio in fetuses of PE mother rats (1.0 vs 0.8 in the control, rabbit serum-treated, PE group; $P=0.03$, Mann-Whitney test, shown median with interquartile range); $n=72$ in the (Continued)

not mention maternal vasculopathy; however, they did not investigate later time points.

The second important finding of our study was the decreased interstitial trophoblast cell invasion in preeclamptic rats with reduced number of NK cells. In humans and rats, trophoblast cells invade the uterine interstitium^{25,26} and the lumina of spiral arteries.^{27,28} In rats, interstitial trophoblast cell invasion occurs after endovascular invasion.²⁵ This finding again supports our hypothesis that the observed vasculopathy occurred at the end of pregnancy, hampering physiological interstitial trophoblast cell invasion and a putative (according to Chakraborty et al¹⁶) increased endovascular trophoblast cell invasion. The increased weight of the uteroplacental unit in anti-asialo GM1-treated preeclamptic rats and especially their increased uteroplacental unit/fetal weight ratio could reflect placental insufficiency as a consequence of decreased trophoblast cell invasion. Traditionally, an increased placental/fetal weight ratio has been used as a marker for an inefficient placenta.²⁹ An alternative way to demonstrate placental insufficiency would be to study umbilical Doppler images, which should be considered in further experiments. The decreased interstitial trophoblast cell invasion is in accordance with earlier work showing that in humans decidual NK cells, but not peripheral blood-derived NK cells, support trophoblast cell invasion and induce angiogenesis in the decidua.³⁰ These processes are 2 important events in early pregnancy. Recently, Kieckbusch et al showed that a major histocompatibility complex-mediated inhibition of uNK cells leads to slightly diminished fetal growth and altered spiral artery remodeling in mice.³¹ Reduction of NK cells did not change spiral artery remodeling in our preeclamptic rats, but we could show a decrease in fetal weight in our wild-type SD rats after NK cell reduction. The mouse model is problematic because murine intrauterine trophoblast cell invasion is shallow³² compared with humans and rats.

Figure 4 Continued. anti-asialo GM1 PE group and $n=55$ in the control, rabbit serum-treated, PE group. **B**, Anti-asialo GM1 application did not change fetal weight in PE mother rats (2.8 vs 2.9 g in the control, rabbit serum-treated group; $P=0.3$, Mann-Whitney test, shown median with interquartile range); $n=73$ in the anti-asialo GM1-treated, PE group and $n=56$ in the control, rabbit serum-treated PE group. **C**, Anti-asialo GM1 treatment of PE rats did not change maternal blood pressure during pregnancy. Blood pressure was measured on 16 days throughout pregnancy, and there was no difference at any time in mean arterial blood pressure between the anti-asialo GM1-treated, PE and the control, rabbit serum-treated PE group (eg, 155 ± 3 vs 158 ± 4 mm

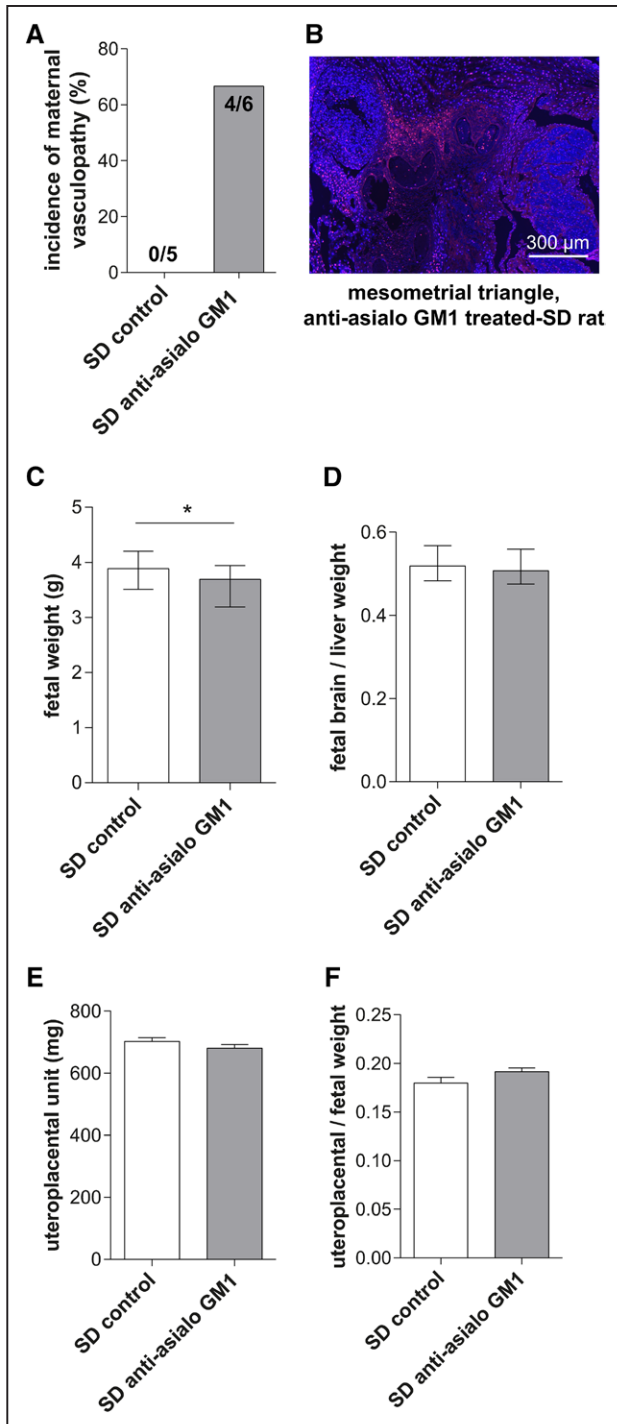


Figure 5. Influence of anti-asialo GM1 on fetal outcome and maternal uterine vessels in wild-type, Sprague-Dawley (SD) rats on pregnancy day 21. **A**, Quantification of maternal vasculopathy in the mesometrial triangle of SD rats on pregnancy day 21: application of anti-asialo GM1 ($n=6$) induced in 4 of 6 SD mother rats (4/6, 66.7%) a vasculopathy (according pictures from Figure 2). There was no vasculopathy in any rabbit serum-treated, SD mother rat ($n=5$, 0/5, 0%). **B**, Terminal deoxynucleotidyl transferase dUTP nick end labeling (TUNEL) assay (red) to detect apoptotic cells with 4',6-diamidino-2-phenylindole staining (blue) for visualization of cell nuclei. Uteroplacental unit of a highly growth-restricted fetus (1.6 g) in a SD mother rat after anti-asialo GM1 application. There is a large area of absent nuclear staining in the middle of the picture. Within this area, there is TUNEL positivity. $\times 10$ magnification. **C**, Anti-asialo (*Continued*)

Natural killer cells are part of the innate immune system and characterized by interferon γ production influencing immune cells of the adaptive immune system. Interestingly, there is increasing evidence that NK cells are related to the growing family of innate lymphoid cells (ILCs).^{33,34} Several ILCs express markers such as Nkp46 that were formerly considered to be exclusively expressed on NK cells.³⁴ ILCs are non-T and non-B cells mirroring functions of T cells but with prompt reaction to antigens or injured tissues.³⁵ Their presence is locally enriched in barrier surfaces.³⁶ On the basis of the signature cytokines they produce,³⁴ there are 3 classes of ILCs (ILC1, ILC2, and ILC3) at the moment. Group 1 consists of interferon- γ -producing cells and thus NK cells are considered to belong to the ILC1 group. However, NK cells can still be distinguished because they display cytotoxicity and because their maturation depends on the transcription factor eomesodermin.^{37,38} Furthermore, the transcriptional program of NK cells differs, at least in parts, from that of ILC1s.³³ Thus, they are still commonly referred to as NK cells.³⁵ Taken together, the quickly emerging, complex types and subtypes of ILCs in addition to their potential for inter-conversion between ILC groups³⁹ make a clear identification of ILC types and their distinction from other immune cells almost impossible with current techniques. Thus far, there has not been any description of ILCs in the rat, but it is likely that they exist there as well. Although we cannot claim that we also reduced ILC1s and other ILCs in our study, we can conclude on the basis of our results and current knowledge that we have reduced what is considered to be NK cells in the spleen and uterus at the moment.

Traditionally, NK cells have been considered as a homogenous lymphocyte population circulating in blood, spleen, and other organs (circulating NK cells). However, there is clear evidence that subtypes of NK cells reside in tissues (tissue-resident NK cells) such as liver, thymus, uterus,⁴⁰ and the salivary gland⁴¹ exhibiting different functions and capabilities. Strikingly, tissue-resident NK cells do not seem to require the NK cell specification transcription factor Nfil3 (nuclear factor interleukin-3-regulated

protein),⁴¹ leading to the assumption that tissue-resident NK cells are distinct from circulating NK cells and could represent a different cell lineage.⁴⁰ The independence of Nfil3 has been shown for uNK cell differentiation in mice as well.⁴² Tissue-resident NK cells in the liver develop independent of eomesodermin,⁴³ whereas tissue-resident NK cells in the uterus highly express eomesodermin,⁴⁴ suggesting more similarities of uNK cells to circulating NK cells. However, the precise origin of uNK cells remains unclear. Nevertheless, tissue-resident NK cells seem to be distinguishable from each other and in parts from ILCs.⁴⁰ Recently, a population of nonkiller uterine ILC3s has been found in human endometrium and decidua.⁴⁵ Rat uNK cells have not well been characterized recently⁴⁶ and, to our knowledge, rat uterine ILCs have never been described.

We used a published, successful protocol to reduce NK cells in rats¹⁶ by administering anti-asialo GM1 antiserum. This antiserum reduces NK cells in almost every organ in the body, including spleen^{16,47} rather than just uNK cells. Moreover, anti-asialo GM1 also reacts with nonparenchymal liver cells,⁴⁸ T cells in mice⁴⁹ and rats,⁵⁰ as well as murine basophils⁵¹ and monocytes⁵² and rat granulocytes and macrophages.⁵⁰ The effect on various ILC subsets is poorly described. Thus, we cannot conclude that the effects we observed were solely the result of NK or even uNK cell reduction. Because the pregnant uterus contains relatively few immune cells with uNK cells representing the major population, we consider a relevant local effect mediated by other cells unlikely. Considering the heterogeneity of uNK cells in mouse and human, the effects of anti-asialo GM1 treatment reported herein may rely on the reduction of one of the subsets. One study found that anti-asialo GM1 does not deplete tissue-resident NK cells in the kidney.⁵³ But within that same article, the authors have shown that uterine tissue-resident NK cells seem to be an exception because they were uniformly expressing high levels of asialo GM1 that was similar to circulating NK cells in some strains.⁵³ Currently, the only way of temporarily depleting or reducing NK cells in the rat is administering antibodies or the antiserum anti-asialo GM1. Other groups have also successfully relied on this approach.^{16,46,54}

We detected an increase in interleukin-15 gene expression in the mesometrial triangles of anti-asialo GM1-treated, preeclamptic rats at the end of pregnancy. In humans, interleukin-15 is expressed by endometrial stromal cells⁵⁵ and involved in recruitment of uNK cells to the endometrium.⁵⁶ One could interpret the increase in interleukin-15 in the mesometrial triangle after NK cell reduction as a homeostatic, compensatory mechanism to replenish the uNK cell population, confirming the successful reduction of NK cells in the uterus.

The importance of uNK cells in the maintenance of pregnancy, particularly in late gestation, is still imperfectly understood.⁵⁷ Earlier animal investigations did not address disease processes such as hypertension in pregnancy or preeclampsia. We found vascular pathology in preeclamptic rats when NK cells are reduced, but we did not observe any effect on blood pressure and albuminuria. The data from our animal model do not support a major role for NK cells in this experimental preeclampsia but definitely indicate an effect on uterine maternal vasculopathy and fetal growth.

Perspectives

An effect of natural killer cells on the preeclamptic phenotype could not be supported by our results. However, their reduction exerts a degenerative vascular effect on the maternal side of the uteroplacental unit that is associated with fetal growth restriction in wild-type rats. These complex results nonetheless direct a therapeutic focus on new targets. Viewing preeclampsia as a NK cell disease in terms of modulation would be a shift from current thinking. Because no therapeutic options have developed for patients, this method of thought could direct future ideas.

Acknowledgments

We thank Juliane Anders, Ute Gerhard, May-Britt Köhler, Reika Langanki, Jutta Meisel, Nancy Mengel, Ralph Plehm, and Astrid Schiche for their excellent technical assistance.

Sources of Funding

M. Golic is participant of the BIH-Charité Clinician Scientist Program funded by the Charité - Universitätsmedizin Berlin and the Berlin Institute of Health. The German Research Foundation (DFG) supported F. Herse (HE 6249/1–2) and R. Dechend (DE 631/9-1). The German Centre for Cardiovascular Research (DZHK) supported D.N. Müller. A.C. Staff, R. Dechend, and P. Alnaes-Katjavivi are supported by the Research Council of Norway and The Regional Health Authorities of South-Eastern Norway.

Disclosures

None.

References

1. Carter AM. Placental circulation. In: Steven DH, ed. *Comparative Placentation: Essays in Structure and Function*. New York, NY: Academic Press; 1975:108–160.
2. Steven D. Anatomy of the placental barrier. In: Steven DH, ed. *Comparative Placentation: Essays in Structure and Function*. New York, NY: Academic Press; 1975:25–57.
3. Steven D, Morris G. Development of the foetal membranes. In: Steven DH, ed. *Comparative Placentation: Essays in Structure and Function*. New York, NY: Academic Press; 1975:58–86.
4. Pijnenborg R, Bland JM, Robertson WB, Brosens I. Uteroplacental arterial changes related to interstitial trophoblast migration in early human pregnancy. *Placenta*. 1983;4:397–413.
5. Pijnenborg R, Vercruyse L, Hanssens M. The uterine spiral arteries in human pregnancy: facts and controversies. *Placenta*. 2006;27:939–958. doi: 10.1016/j.placenta.2005.12.006.
6. Sibai B, Dekker G, Kupferminc M. Pre-eclampsia. *Lancet*. 2005;365:785–799. doi: 10.1016/S0140-6736(05)17987-2.
7. Powe CE, Ecker J, Rana S, Wang A, Ankers E, Ye J, Levine RJ, Karumanchi SA, Thadhani R. Preeclampsia and the risk of large-for-gestational-age infants. *Am J Obstet Gynecol*. 2011;204:425.e1–425.e6. doi: 10.1016/j.ajog.2010.12.030.
8. Irgens HU, Reisaeter L, Irgens LM, Lie RT. Long term mortality of mothers and fathers after pre-eclampsia: population based cohort study. *BMJ*. 2001;323:1213–1217.
9. Barker DJ, Fall CH. Fetal and infant origins of cardiovascular disease. *Arch Dis Child*. 1993;68:797–799.
10. Redman CW, Sargent IL. Latest advances in understanding preeclampsia. *Science*. 2005;308:1592–1594. doi: 10.1126/science.1111726.
11. Redman CW, Sargent IL. Immunology of pre-eclampsia. *Am J Reprod Immunol*. 2010;63:534–543. doi: 10.1111/j.1600-0897.2010.00831.x.
12. Lash GE, Robson SC, Bulmer JN. Review: functional role of uterine natural killer (uNK) cells in human early pregnancy decidua. *Placenta*. 2010;31(suppl):S87–S92. doi: 10.1016/j.placenta.2009.12.022.
- 13.

14. King A, Birkby C, Loke YW. Early human decidual cells exhibit NK activity against the K562 cell line but not against first trimester trophoblast. *Cell Immunol.* 1989;118:337–344.
15. Wilczyński JR, Tchórzewski H, Banasik M, Głowacka E, Wieczorek A, Lewkowicz P, Malinowski A, Szpakowski M, Wilczyński J. Lymphocyte subset distribution and cytokine secretion in third trimester decidua in normal pregnancy and preeclampsia. *Eur J Obstet Gynecol Reprod Biol.* 2003;109:8–15.
16. Chakraborty D, Rumi MA, Konno T, Soares MJ. Natural killer cells direct hemochorial placentation by regulating hypoxia-inducible factor dependent trophoblast lineage decisions. *Proc Natl Acad Sci USA.* 2011;108:16295–16300. doi: 10.1073/pnas.1109478108.
17. Redman CW, Sargent IL, Staff AC. IFPA Senior Award Lecture: making sense of pre-eclampsia - two placental causes of preeclampsia? *Placenta.* 2014;35(suppl):S20–S25. doi: 10.1016/j.placenta.2013.12.008.
18. Dechend R, Gratz P, Wallukat G, Shagdarsuren E, Plehm R, Bräsen JH, Fiebeler A, Schneider W, Caluwaerts S, Vercruyse L, Pijnenborg R, Luft FC, Müller DN. Agonistic autoantibodies to the AT1 receptor in a transgenic rat model of preeclampsia. *Hypertension.* 2005;45:742–746. doi: 10.1161/01.HYP.0000154785.50570.63.
19. Takimoto E, Ishida J, Sugiyama F, Horiguchi H, Murakami K, Fukamizu A. Hypertension induced in pregnant mice by placental renin and maternal angiotensinogen. *Science.* 1996;274:995–998.
20. Verlohren S, Niehoff M, Hering L, Geusens N, Herse F, Tintu AN, Plagemann A, LeNoble F, Pijnenborg R, Muller DN, Luft FC, Dudenhausen JW, Gollasch M, Dechend R. Uterine vascular function in a transgenic preeclampsia rat model. *Hypertension.* 2008;51:547–553. doi: 10.1161/HYPERTENSIONAHA.107.103176.
21. Geusens N, Hering L, Verlohren S, Luyten C, Drijkoningen K, Taube M, Vercruyse L, Hanssens M, Dechend R, Pijnenborg R. Changes in endovascular trophoblast invasion and spiral artery remodelling at term in a transgenic preeclamptic rat model. *Placenta.* 2010;31:320–326. doi: 10.1016/j.placenta.2010.01.011.
22. Geusens N, Verlohren S, Luyten C, Taube M, Hering L, Vercruyse L, Hanssens M, Dudenhausen JW, Dechend R, Pijnenborg R. Endovascular trophoblast invasion, spiral artery remodelling and uteroplacental haemodynamics in a transgenic rat model of pre-eclampsia. *Placenta.* 2008;29:614–623. doi: 10.1016/j.placenta.2008.04.005.
23. Guimond MJ, Luross JA, Wang B, Terhorst C, Danial S, Croy BA. Absence of natural killer cells during murine pregnancy is associated with reproductive compromise in TgE26 mice. *Biol Reprod.* 1997;56:169–179.
24. Hofmann AP, Gerber SA, Croy BA. Uterine natural killer cells pace early development of mouse decidua basalis. *Mol Hum Reprod.* 2014;20:66–76. doi: 10.1093/molehr/gat060.
25. Vercruyse L, Caluwaerts S, Luyten C, Pijnenborg R. Interstitial trophoblast invasion in the decidua and mesometrial triangle during the last third of pregnancy in the rat. *Placenta.* 2006;27:22–33. doi: 10.1016/j.placenta.2004.11.004.
26. Al-Nasiry S, Vercruyse L, Hanssens M, Luyten C, Pijnenborg R. Interstitial trophoblastic cell fusion and E-cadherin immunostaining in the placental bed of normal and hypertensive pregnancies. *Placenta.* 2009;30:719–725. doi: 10.1016/j.placenta.2009.05.006.
27. Pijnenborg R. Uterine haemodynamics as a possible driving force for endovascular trophoblast migration in the placental bed. *Med Hypotheses.* 2000;55:114–118. doi: 10.1054/mehy.1999.1040.
28. Caluwaerts S, Vercruyse L, Luyten C, Pijnenborg R. Endovascular trophoblast invasion and associated structural changes in uterine spiral arteries of the pregnant rat. *Placenta.* 2005;26:574–584. doi: 10.1016/j.placenta.2004.09.007.
29. Salafia CM, Charles AK, Maas EM. Placenta and fetal growth restriction. *Clin Obstet Gynecol.* 2006;49:236–256.
30. Hanna J, Goldman-Wohl D, Hamani Y, et al. Decidual NK cells regulate key developmental processes at the human fetal-maternal interface. *Nat Med.* 2006;12:1065–1074. doi: 10.1038/nm1452.
31. Kieckbusch J, Gaynor LM, Moffett A, Colucci F. MHC-dependent inhibition of uterine NK cells impedes fetal growth and decidual vascular remodelling. *Nat Commun.* 2014;5:3359. doi: 10.1038/ncomms4359.
32. Ain R, Canham LN, Soares MJ. Gestation stage-dependent intrauterine trophoblast cell invasion in the rat and mouse: novel endocrine phenotype and regulation. *Dev Biol.* 2003;260:176–190.
33. Robinette ML, Fuchs A, Cortez VS, Lee JS, Wang Y, Durum SK, Gilfillan S, Colonna M; Immunological Genome Consortium. Transcriptional programs define molecular characteristics of innate lymphoid cell classes and subsets. *Nat Immunol.* 2015;16:306–317. doi: 10.1038/ni.3094.
34. Spits H, Artis D, Colonna M, Dieffenbach A, Di Santo JP, Eberl G, Koyasu S, Locksley RM, McKenzie AN, Mebius RE, Powrie F, Vivier E. Innate lymphoid cells—a proposal for uniform nomenclature. *Nat Rev Immunol.* 2013;13:145–149. doi: 10.1038/nri3365.
35. Eberl G, Colonna M, Di Santo JP, McKenzie AN. Innate lymphoid cells. Innate lymphoid cells: a new paradigm in immunology. *Science.* 2015;348:aaa6566. doi: 10.1126/science.aaa6566.
36. Dieffenbach A, Colonna M, Koyasu S. Development, differentiation, and diversity of innate lymphoid cells. *Immunity.* 2014;41:354–365. doi: 10.1016/j.immuni.2014.09.005.
37. Klose CS, Flach M, Möhle L, et al. Differentiation of type 1 ILCs from a common progenitor to all helper-like innate lymphoid cell lineages. *Cell.* 2014;157:340–356. doi: 10.1016/j.cell.2014.03.030.
38. Gordon SM, Chaix J, Rupp LJ, Wu J, Madera S, Sun JC, Lindsten T, Reiner SL. The transcription factors T-bet and Eomes control key checkpoints of natural killer cell maturation. *Immunity.* 2012;36:55–67. doi: 10.1016/j.immuni.2011.11.016.
39. Cella M, Otero K, Colonna M. Expansion of human NK-22 cells with IL-7, IL-2, and IL-1beta reveals intrinsic functional plasticity. *Proc Natl Acad Sci USA.* 2010;107:10961–10966. doi: 10.1073/pnas.1005641107.
40. Sojka DK, Plougastel-Douglas B, Yang L, Pak-Wittel MA, Artymov MN, Ivanova Y, Zhong C, Chase JM, Rothman PB, Yu J, Riley JK, Zhu J, Tian Z, Yokoyama WM. Tissue-resident natural killer (NK) cells are cell lineages distinct from thymic and conventional splenic NK cells. *Elife.* 2014;3:e01659.
41. Cortez VS, Fuchs A, Cella M, Gilfillan S, Colonna M. Cutting edge: salivary gland NK cells develop independently of Nfil3 in steady-state. *J Immunol.* 2014;192:4487–4491. doi: 10.4049/jimmunol.1303469.
42. Redhead ML, Portilho NA, Felker AM, Mohammad S, Mara DL, Croy BA. The transcription factor NFIL3 is essential for normal placental and embryonic development but not for uterine natural killer (UNK) cell differentiation in mice. *Biol Reprod.* 2016;94:101. doi: 10.1095/biolreprod.116.138495.
43. Daussy C, Faure F, Mayol K, et al. T-bet and Eomes instruct the development of two distinct natural killer cell lineages in the liver and in the bone marrow. *J Exp Med.* 2014;211:563–577. doi: 10.1084/jem.20131560.
44. Tayade C, Fang Y, Black GP, V A P Jr, Erlebacher A, Croy BA. Differential transcription of Eomes and T-bet during maturation of mouse uterine natural killer cells. *J Leukoc Biol.* 2005;78:1347–1355. doi: 10.1189/jlb.0305142.
45. Doisne JM, Balmes E, Boulenouar S, Gaynor LM, Kieckbusch J, Gardner L, Hawkes DA, Barbara CF, Sharkey AM, Brady HJ, Brosens JJ, Moffett A, Colucci F. Composition, development, and function of uterine innate lymphoid cells. *J Immunol.* 2015;195:3937–3945. doi: 10.4049/jimmunol.1500689.
46. Head JR, Kresge CK, Young JD, Hiserodt JC. NKR-P1+ cells in the rat uterus: granulated metrial gland cells are of the natural killer cell lineage. *Biol Reprod.* 1994;51:509–523.
47. Monnier J, Zabel BA. Anti-asialo GM1 NK cell depleting antibody does not alter the development of bleomycin induced pulmonary fibrosis. *PLoS One.* 2014;9:e99350. doi: 10.1371/journal.pone.0099350.
48. Cohen SA, Tzung SP, Doerr RJ, Goldrosen MH. Role of asialo-GM1 positive liver cells from athymic nude or polyinosinic-polycytidylic acid-treated mice in suppressing colon-derived experimental hepatic metastasis. *Cancer Res.* 1990;50:1834–1840.
49. Moore ML, Chi MH, Goleniewska K, Durbin JE, Peebles RS Jr. Differential regulation of GM1 and asialo-GM1 expression by T cells and natural killer (NK) cells in respiratory syncytial virus infection. *Viral Immunol.* 2008;21:327–339. doi: 10.1089/vim.2008.0003.
50. Momoi T, Nakajima K, Sakakibara K, Nagai Y. Localization of a glycosphingolipid, asialo GM1, in rat immunocytes. *J Biochem.* 1982;91:301–310.
51. Nishikado H, Mukai K, Kawano Y, Minegishi Y, Karasuyama H. NK cell-depleting anti-asialo GM1 antibody exhibits a lethal off-target effect on basophils in vivo. *J Immunol.* 2011;186:5766–5771. doi: 10.4049/jimmunol.1100370.
52. Shimamura K, Habu S, Fukui H, Akatsuka A, Okumura K, Tamaoki N. Morphology and function of ganglio-N-tetraosylceramide-positive lymphocyte mediators of natural killer activity. *J Natl Cancer Inst.* 1982;68:449–455.
- 53.

54. Tsuchida T, Zheng YW, Zhang RR, Takebe T, Ueno Y, Sekine K, Taniguchi H. The development of humanized liver with Rag1 knock-out rats. *Transplant Proc.* 2014;46:1191–1193. doi: 10.1016/j.transproceed.2013.12.026.
55. Kitaya K, Yasuda J, Yagi I, Tada Y, Fushiki S, Honjo H. IL-15 expression at human endometrium and decidua. *Biol Reprod.* 2000;63:683–687.
56. Kitaya K, Yamaguchi T, Honjo H. Central role of interleukin-15 in post-ovulatory recruitment of peripheral blood CD16(-) natural killer cells into human endometrium. *J Clin Endocrinol Metab.* 2005;90:2932–2940. doi: 10.1210/jc.2004-2447.
- 57.

Novelty and Significance

What Is New?

- We report the first interventional study of reducing natural killer cells in an established rat model for preeclampsia.
- Substantial reduction of natural killer cells is not altering the preeclamptic phenotype.
- We are the first to describe that reduction of natural killer cells induces maternal uterine vasculopathy in hypertensive rat pregnancy.

What Is Relevant?

- In preeclamptic rats, reduction of natural killer cells alters the uteroplacental unit with a decrease in interstitial trophoblast cell invasion and an induction of maternal vasculopathy with degenerative vessels exhibiting

excessive fibrosis, but it did not modify maternal hypertension and albuminuria. In wild-type rats, reduction of natural killer cells also induces maternal uterine vasculopathy, which is associated with fetal growth restriction. The work directs attention to a different and novel aspect of immunology.

Summary

This study demonstrates a role for natural killer cells in trophoblast cell invasion and in maintenance of vascular integrity in the uterus needed for fetal growth.

Hypertension

JOURNAL OF THE AMERICAN HEART ASSOCIATION



Natural Killer Cell Reduction and Uteroplacental Vasculopathy

Michaela Golic, Nadine Haase, Florian Herse, Anika Wehner, Lisbeth Vercruysse, Robert Pijnenborg, Andras Balogh, Per Christian Saether, Erik Dissen, Friedrich C. Luft, Lukasz Przybyl, Joon-Keun Park, Patji Alnaes-Katjavivi, Anne Cathrine Staff, Stefan Verlohren, Wolfgang Henrich, Dominik N. Muller and Ralf Dechend

Hypertension. published online August 22, 2016;

Hypertension is published by the American Heart Association, 7272 Greenville Avenue, Dallas, TX 75231

Copyright © 2016 American Heart Association, Inc. All rights reserved.

Print ISSN: 0194-911X. Online ISSN: 1524-4563

The online version of this article, along with updated information and services, is located on the World Wide Web at:

<http://hyper.ahajournals.org/content/early/2016/08/22/HYPERTENSIONAHA.116.07800>

Data Supplement (unedited) at:

<http://hyper.ahajournals.org/content/suppl/2016/08/22/HYPERTENSIONAHA.116.07800.DC1>

ONLINE SUPPLEMENT

NATURAL KILLER CELL REDUCTION AND UTEROPLACENTAL VASCULOPATHY

Short title: NK cells and uteroplacental vasculopathy

Michaela Golic^{1,2,3}, Nadine Haase^{1,3,4}, Florian Herse^{1,3,4}, Anika Wehner^{1,3,5}, Lisbeth Vercruysse⁶, Robert Pijnenborg⁶, Andras Balogh^{1,3,4,7}, Per Christian Saether^{8,9}, Erik Dissen⁸, Friedrich C. Luft^{1,3,5}, Lukasz Przybyl^{1,3,5}, Joon-Keun Park¹⁰, Patji Alnaes-Katjavivi^{11,12}, Anne Cathrine Staff^{11,12}, Stefan Verlohren^{3,13}, Wolfgang Henrich¹³, Dominik N. Müller^{1,3,4}, Ralf Dechend^{1,3,5,14}

¹ Experimental and Clinical Research Center, a cooperation between the Max Delbrück Center for Molecular Medicine in the Helmholtz Association and the Charité - Universitätsmedizin Berlin, Berlin, Germany.

² Department of Obstetrics and Department of Gynecology, Charité - Universitätsmedizin Berlin, Berlin, Germany.

³ Berlin Institute of Health (BIH), Berlin, Germany

⁴ Max Delbrück Center for Molecular Medicine in the Helmholtz Association, Berlin, Germany

⁵ Charité - Universitätsmedizin Berlin, Campus Berlin Buch, Berlin, Germany

⁶ Department of Development and Regeneration, University Hospital Leuven, Leuven, Belgium.

⁷ Department of Medical Biology, János Szentágothai Research Centre Pécs, University of Pécs Medical School, Pécs, Hungary.

⁸ Department of Molecular Medicine, Institute of Basic Medical Sciences, University of Oslo, Oslo, Norway

⁹ Department of Multi-Disciplinary Laboratory Medicine and Medical Biochemistry, Akershus University Hospital, Lørenskog, Norway

¹⁰ Clinic for Nephrology and Hypertension, Hannover Medical School, Hannover, Germany.

¹¹ University of Oslo, Oslo, Norway.

¹² Departments of Obstetrics and Gynecology, Oslo University Hospital, Oslo, Norway.

¹³ Department of Obstetrics, Charité - Universitätsmedizin Berlin, Berlin, Germany.

¹⁴ Department of Cardiology and Nephrology, HELIOS Klinikum Berlin, Berlin, Germany.

Correspondence:

Ralf Dechend, MD

Experimental and Clinical Research Center

Lindenberger Weg 80

13125 Berlin, Germany

Phone: +49 30-450-540-303

Fax: +49 30-450-540-944

E-mail: ralf.dechend@charite.de

Materials and Methods

Animals and procedures

Local German authorities approved the studies that were conducted in accordance with the National Institutes of Health (NIH) guide for the care and use of laboratory animal standards. Our model involves two Sprague-Dawley rat lines: female rats expressing the human angiotensinogen (hAOGEN) and male rats expressing the human renin (hREN) gene. After mating, the dam develops severe hypertension¹ and some target organ damage in the second half of pregnancy.² At the end of pregnancy, the fetuses exhibit low birth weight and increased brain/liver weight ratio compared to normal non-transgenic Sprague-Dawley offspring confirming intrauterine growth restriction.³ The placentas in preeclamptic (PE) dams are lighter than those in control rats.⁴ Together with the group of Robert Pijnenborg, we had investigated the uteroplacental unit in this model and had shown a pathological endovascular trophoblast cell invasion with an altered uteroplacental vascular remodeling.⁵⁻⁷ Ganglio-N-tetraosylceramide (asialo GM1) is a glycolipid expressed on natural killer cells (NK cells) in mice,⁸ rats,⁹ and humans.¹⁰ The antiserum anti-asialo GM1 successfully depletes NK cells in mice⁸ and rats.¹¹ It also depletes uterine NK cells (uNK cells).¹¹ We administered 0.5 ml rabbit anti-asialo GM1 antiserum (Wako Pure Chemical Industries) to pregnant dams intraperitoneally on day 5 and day 10 of pregnancy according to a protocol published by other investigators earlier.¹¹ Pregnancy day 1 was defined by the presence of a vaginal copulation plug. Control PE rats received 0.5 ml rabbit serum (Jackson ImmunoResearch Laboratories). Rats from each group were anesthetized and euthanized for analysis either on day 15 or day 21 of pregnancy. Preeclamptic pregnant rats observed until pregnancy day 21 received continuous blood pressure monitoring by radiotelemetry (Data Science International). In healthy wild type Sprague-Dawley rats (SD), blood pressure was obtained by tail cuff measurement on pregnancy days 5, 10, 15/16, and 20/21. For quantification of 24 hours albumin excretion, rats were placed in metabolic cages and urine was collected (on pregnancy day 18/19 in PE rats, and on pregnancy day 17/18 in SD rats). Urinary albumin excretion was analyzed by ELISA (CellTrend). Serum cystatin C was determined by ELISA (BioVendor) according to manufacturer's protocol. Serum creatinine was assessed by an automated clinical method (HELIOS Klinikum Berlin-Buch). In our study, we examined two different rat strains, transgenic PE Sprague-Dawley rats and healthy wild type SD rats. Maternal blood pressure, albuminuria, fetal and uteroplacental weights and ratios, and analysis of uterine vasculopathy has been evaluated in PE mother rats (n=7 anti-asialo GM1-treated rats and n=5 normal rabbit serum-treated rats) and SD mother rats (n=6 or 7 anti-asialo GM1-treated rats and n=5 or 6 normal rabbit serum-treated rats) on pregnancy day 21. Proof of NK cell reduction has been performed in PE rats on pregnancy day 15 (flow cytometry spleen: n=3 anti-asialo GM1-treated rats and n=3 normal rabbit serum-treated rats; histology uterus: n=3 anti-asialo GM1-treated rats and n=3 normal rabbit serum-treated rats; gene expression uterus: n=2 anti-asialo GM1-treated rats and n=4 normal rabbit serum-treated rats). Histological evaluation of trophoblast cell invasion and spiral artery remodeling has been performed in PE rats on pregnancy day 21 (n=8 uteroplacental units out of 7 anti-asialo GM1-treated rats and n=5 uteroplacental units out of 5 normal rabbit serum-treated rats). Maternal angiogenic profilin in plasma has been evaluated in PE rats on pregnancy day 21 (n=7 anti-asialo GM1-treated rats and n=5 normal rabbit serum-treated rats). Gene expression of interleukin 15 in the uteroplacental unit has been analyzed in PE rats on pregnancy day 21 (n=5 out of 7 anti-asialo GM1-treated rats and n=5 out of 5 normal rabbit serum-treated rats). Angiogenic profilin of the uteroplacental unit has been analyzed in PE rats on pregnancy day 21. Maternal serum creatinine, cystatin C, and body weight has

been evaluated in PE rats on pregnancy day 21 (n=7 anti-asialo GM1-treated rats and n=4 or 5 normal rabbit serum-treated)

RNA isolation, reverse transcription polymerase chain reaction and protein isolation

We isolated total mRNA from mesometrial triangle and placentas (together called uteroplacental unit) using QIAzol Lysis Reagent, RNeasy Mini Kit, and RNase-Free DNase Set (all Qiagen) according to the manufacturer's protocol. Then, RNA was transcribed into cDNA by the High-Capacity cDNA Reverse Transcription Kit (Applied Biosystems) with a DNA Thermal Cycler (Perkin Elmer) and analyzed in triplicates by real time quantitative polymerase chain reaction on 7500 Fast Real-Time PCR System (Applied Biosystem). Results were normalized to 18s. We designed our primers and probes (BioTeZ Berlin Buch GmbH) with Primer Express 3.0 (Applied Biosystems). Sequences are listed in the Supplementary Table S1. Proteins were isolated by homogenization in radioimmunoprecipitation assay buffer (RIPA buffer) supplemented with proteinase inhibitors. The placental like growth factor (PLGF) protein concentration was measured with the mouse PLGF-2 Quantikine ELISA Kit (R&D Systems), the soluble fms-like tyrosine kinase 1 (sFLT-1) protein concentration with the rat sFLT-1 ELISA Kit (MyBioSource).

Flow cytometry

Preeclamptic rats having received anti-asialo GM1 (n=3) or normal rabbit serum (n=3), respectively, on pregnancy days 5 and 10 were euthanized on pregnancy day 15. Spleen was removed and a single cell suspension established by mechanical disintegration. After incubation in erythrolysis buffer (NH₄Cl, NaHCO₃, EDTA) cells were labeled with fluorescein isothiocyanate (FITC)-conjugated mouse anti-rat CD161 (mouse IgG1 κ , clone 10/78, Biolegend, CA, USA) and allophycocyanin (APC)-conjugated mouse anti-rat CD3 (clone 1F4, BD Pharmingen™). For isotype control, cells were stained with FITC-conjugated mouse IgG1 κ (clone MOPC-21, BioLegend). Flow cytometry was performed with a BD FACSCanto™ II (BD Biosciences). Data were analyzed with Flow Jo (Tree Star Inc.). Quantification of NK cells was performed on the lymphocyte population.

Tissue preparations

We worked according to a published protocol with minor modifications.⁶ After the rats were sacrificed, placentas and associated mesometrial triangles were removed and fixed for 48 hours at room temperature in a fixative according to Backstead,¹² which is a zinc-based formaldehyde-free fixative consisting of Tris(hydroxymethyl)-aminomethan-buffered calcium acetate (0.05%), zinc acetate (0.5%), and zinc chloride (0.5%). After fixation, the uteroplacental units were transferred to 70% ethanol and embedded in paraffin according to standard procedures. Then several series of ten parallel sections were cut from each uteroplacental unit. The distance between two series was at least 100 μ m. Every section was 3 – 5 μ m thick. For further analysis, we selected one set displaying the most central parts of the uteroplacental unit. Within this set, a Masson-Goldner trichrome staining was performed. Additionally, parallel sections were stained with Periodic Acid Schiff (PAS; for general morphological evaluation and detection of fibrinoid), α -actin (marker for vascular smooth muscle cells, VSMC), cytokeratin (marker for trophoblast cells), CD31 (marker for endothelial cells), and Anti-Natural Killer Cell Activation Structures (ANK61, marker for NK cells; abcam).

Immunohistochemistry and quantitative analysis of trophoblast cells

We applied a protocol published earlier.⁶ We used non-conjugated goat anti-mouse immunoglobulins (Acris Antibodies) at a final dilution 1:50 and mounted the stained sections

in Depex mounting medium (VWR international GmbH) or Aqua-Poly/Mount (Polysciences, Inc.), respectively.

We worked with the program AxioVision 4.1 linked to our Zeiss microscope Axio Imager M2 fitted with a camera AxioCam HRc (all Zeiss). Overview images of the whole uteroplacental unit were developed by using the module 'panorama' (Zeiss). Areas of mesometrial triangle and interstitial trophoblast cell invasion into mesometrial triangle were measured on the overview picture of the most central part of the uteroplacental unit with the module 'interactive measurements' (Zeiss). The mesometrial triangle was defined as the uterine tissue between the two uterine muscle layers. Numbers of trophoblast cells invading into the mesometrial triangle were semiquantitatively evaluated by counting trophoblast cells in microscopic fields at 40 x magnification. We only evaluated microscopic fields containing exclusively mesometrial triangle tissue without large blood vessels and according to availability, four to six randomly assigned fields were evaluated per uteroplacental unit without differentiation between interstitial and endovascular trophoblast cells. Counts of 42 microscopic fields totalized from all anti-asialo GM1-treated uteroplacental units were compared to counts from 29 microscopic fields totalized from all control rabbit serum-treated uteroplacental units. Endovascular trophoblast cell invasion was evaluated by examining every endovascularly invaded spiral artery cross section within the mesometrial triangle. The extension of endovascular trophoblast cell invasion was evaluated by scoring the percentage of vessel lumen circumference infiltrated by trophoblast cells as indicated by cytokeratin positivity (1 point: 0-25%; 2 points: 26-50%; 3 point: 51-75%; 4 points: 76-100%). In case of very low and/or very thin antigen positivity (for cytokeratin), we diminished the score by one. Scores of spiral artery cross sections from all anti-asialo GM1-treated uteroplacental units (n=271 from 8 uteroplacental units) were compared to scores from all control rabbit serum-treated uteroplacental units (n=188 from 5 uteroplacental units). The same score and analysis were applied to investigate the amount of smooth muscle cell tissue within the vessel wall. We interpreted a lower score (representing loss of smooth muscle cells) as vascular remodeling of the spiral artery.

References

1. Bohlender J, Ganten D, Luft FC. Rats transgenic for human renin and human angiotensinogen as a model for gestational hypertension. *Journal Of The American Society Of Nephrology : JASN*. 2000;11:2056-2061.
2. Dechend R, Gratze P, Wallukat G, Shagdarsuren E, Plehm R, Brasen JH, Fiebeler A, Schneider W, Caluwaerts S, Vercruysse L, Pijnenborg R, Luft FC, Muller DN. Agonistic autoantibodies to the AT1 receptor in a transgenic rat model of preeclampsia. *Hypertension*. 2005;45:742-746.
3. Verlohren S, Niehoff M, Hering L, Geusens N, Herse F, Tintu AN, Plagemann A, LeNoble F, Pijnenborg R, Muller DN, Luft FC, Dudenhausen JW, Gollasch M, Dechend R. Uterine vascular function in a transgenic preeclampsia rat model. *Hypertension*. 2008;51:547-553.
4. Hering L, Herse F, Geusens N, Verlohren S, Wenzel K, Staff AC, Brosnihan KB, Huppertz B, Luft FC, Muller DN, Pijnenborg R, Cartwright JE, Dechend R. Effects of circulating and local uteroplacental angiotensin II in rat pregnancy. *Hypertension*. 2010;56:311-318.
5. Geusens N, Hering L, Verlohren S, Luyten C, Drijkoningen K, Taube M, Vercruysse L, Hanssens M, Dechend R, Pijnenborg R. Changes in endovascular trophoblast invasion and spiral artery remodelling at term in a transgenic preeclamptic rat model. *Placenta*. 2010;31:320-326.

6. Geusens N, Verlohren S, Luyten C, Taube M, Hering L, Vercruyssen L, Hanssens M, Dudenhausen JW, Dechend R, Pijnenborg R. Endovascular trophoblast invasion, spiral artery remodelling and uteroplacental haemodynamics in a transgenic rat model of pre-eclampsia. *Placenta*. 2008;29:614-623.
7. Verlohren S, Geusens N, Morton J, Verhaegen I, Hering L, Herse F, Dudenhausen JW, Muller DN, Luft FC, Cartwright JE, Davidge ST, Pijnenborg R, Dechend R. Inhibition of trophoblast-induced spiral artery remodeling reduces placental perfusion in rat pregnancy. *Hypertension*. 2010;56:304-310.
8. Young WW, Jr., Hakomori SI, Durdik JM, Henney CS. Identification of ganglio-N-tetraosylceramide as a new cell surface marker for murine natural killer (NK) cells. *J Immunol*. 1980;124:199-201.
9. Reynolds CW, Sharrow SO, Ortaldo JR, Herberman RB. Natural killer activity in the rat. II. Analysis of surface antigens on LGL by flow cytometry. *J Immunol*. 1981;127:2204-2208.
10. Ortaldo JR, Sharrow SO, Timonen T, Herberman RB. Determination of surface antigens on highly purified human NK cells by flow cytometry with monoclonal antibodies. *J Immunol*. 1981;127:2401-2409.
11. Chakraborty D, Rumi MA, Konno T, Soares MJ. Natural killer cells direct hemochorial placentation by regulating hypoxia-inducible factor dependent trophoblast lineage decisions. *Proceedings Of The National Academy Of Sciences Of The United States Of America*. 2011;108:16295-16300.
12. Beckstead JH. A simple technique for preservation of fixation-sensitive antigens in paraffin-embedded tissues. *The Journal Of Histochemistry And Cytochemistry : Official Journal Of The Histochemistry Society*. 1994;42:1127-1134.

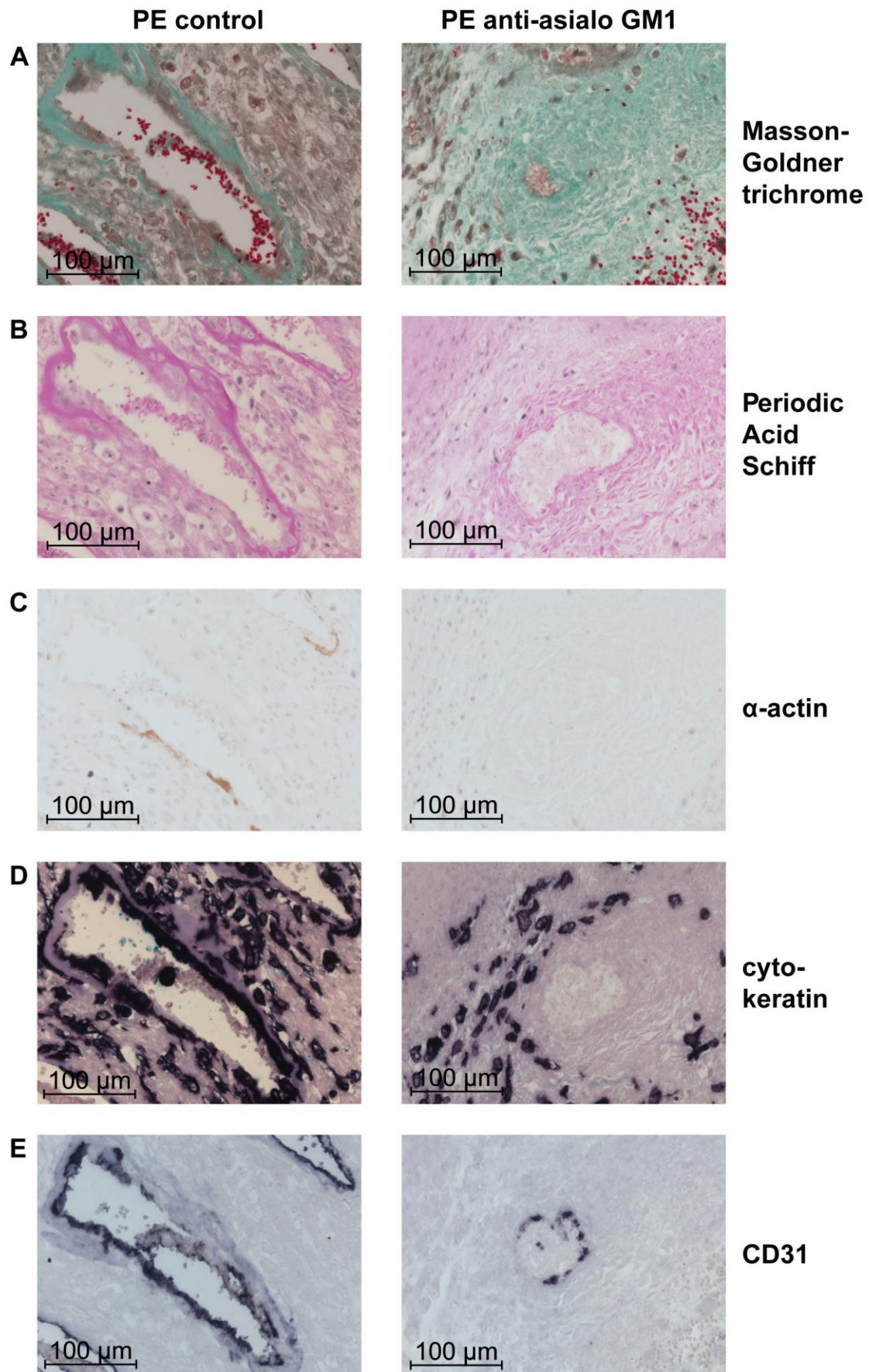
Supplementary Table S1: Primer sequences for quantitative real-time reverse transcription polymerase chain reaction

Gene	Primer	Sequence
rat 18s	forward	5' ACATCCAAGGAAGGCAGCAG 3'
	reverse	5' TTTTCGTCACTACCTCCCCG 3'
	probe	5' FAM-CGCGCAAATTACCCACTCCCGAC-TAMRA 3'
rat IL-15 [#]	forward	5' TGTACTACCTGTGTTTCCTTCTCAACA 3'
	reverse	5' CACTGACACAGCCCAAATGA 3'
	probe	5' FAM-CACTTCTTAACTGAGGCTGGCATCCATGTC-TAMRA 3'
rat NCR1 [*]	forward	5' CATCACAGGAGAGGTTGAGAACAC 3
	reverse	5' GGTCAAACCTCCCAATAATCAAGAGA 3'
	probe	5' FAM-AGCCTTGCACCCACAGACCCTGTTTC-TAMRA 3

[#] interleukin 15

^{*} NCR1: natural cytotoxicity receptor 1

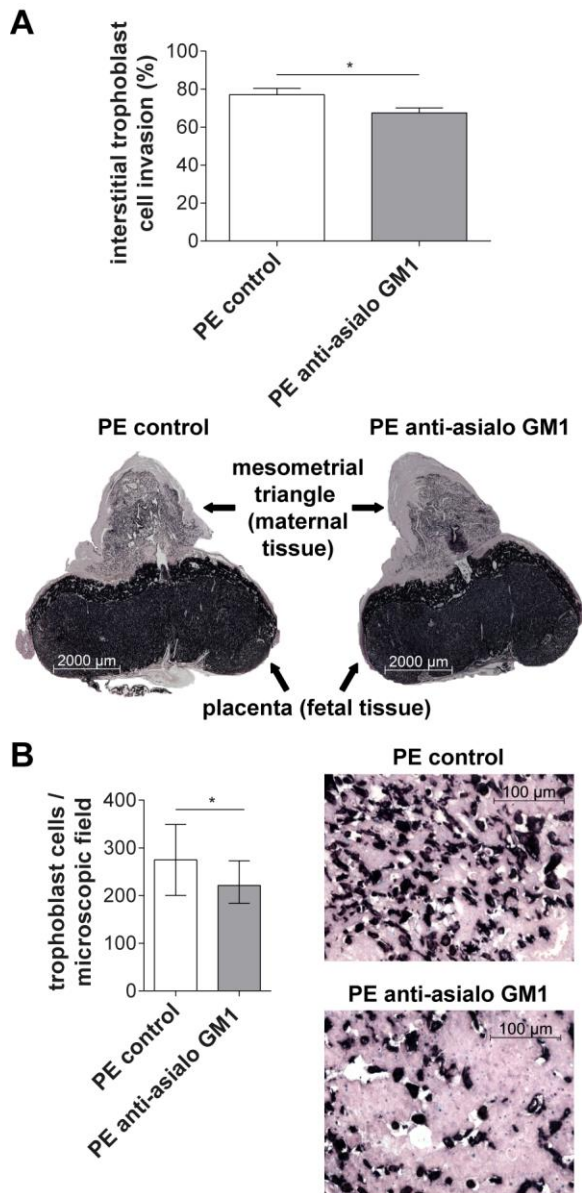
Supplementary Figure S1:



Supplementary Figure S1: Influence of anti-asialo GM1 on maternal uterine vessels in preeclamptic rats (PE) on pregnancy day 21

Degenerative maternal vasculopathy in the mesometrial triangle of PE rats. Same vessels as in Figure 2, but here shown in 40 x magnification. Explanations please see legend to Figure 2.

Supplementary Figure S2:



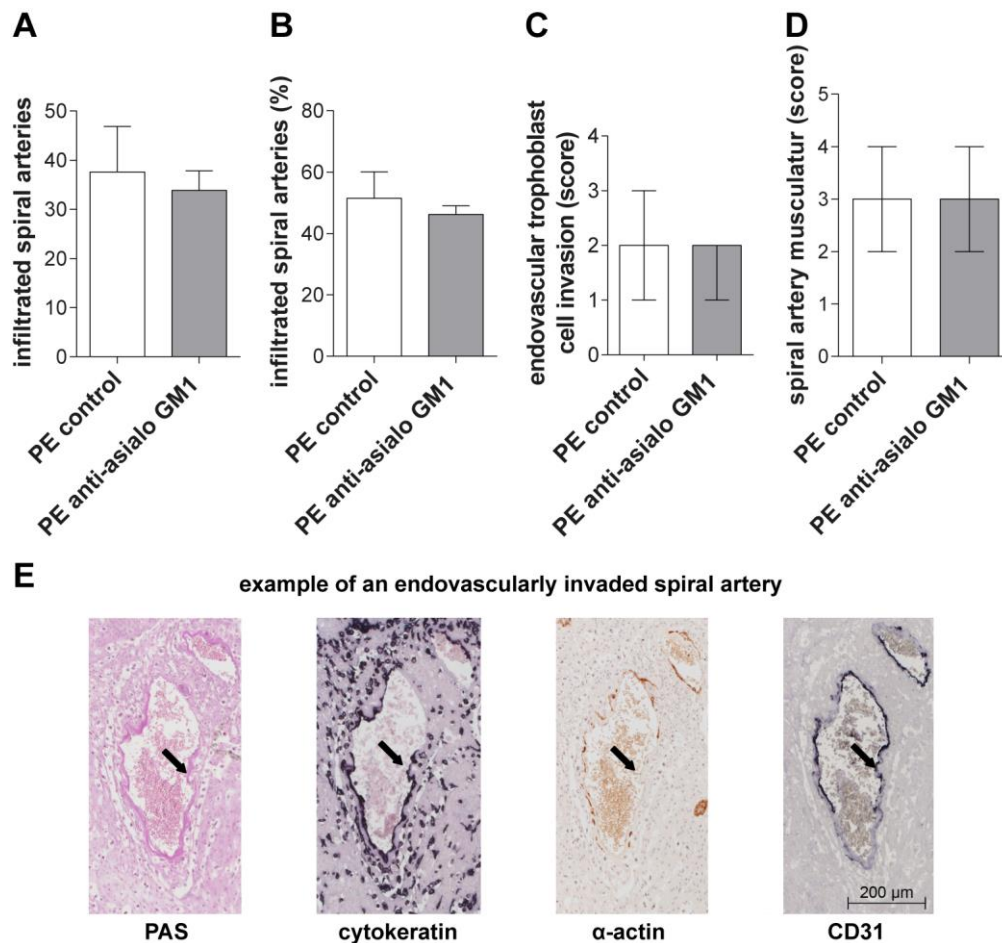
Supplementary Figure S2: Influence of anti-asialo GM1 on interstitial trophoblast cell invasion in preeclamptic rats (PE) on pregnancy day 21

A: Anti-asialo GM1 decreased the area of interstitial trophoblast cell invasion into mesometrial triangle in PE rats ($68 \pm 3\%$ in the anti-asialo GM1 PE group vs. $77 \pm 3\%$ in the control rabbit serum PE group; $p=0.045$, unpaired t-test, shown mean with SEM). The two pictures below show uteroplacental units consisting of placenta (=fetal part; below) and mesometrial triangle (=maternal part; above). It is a cytokeratin staining of trophoblast cells, which appear in black dark after nitro-blue tetrazolium chloride (NBT) and 5-bromo-4-chloro-3'-indolyphosphate p-toluidine salt (BCIP) staining and counterstaining with Periodic Acid Schiff (PAS) and hematoxylin, 10 x magnification.

B: The number of invading trophoblast cells in the mesometrial triangle was decreased in anti-asialo GM1-treated PE rats (221 cells per microscopic field in 40 x magnification vs. 275 cells in the control rabbit serum PE group; $p=0.0493$, Mann Whitney test, shown median with interquartile range). Shown are two exemplary pictures of trophoblast cells in the mesometrial triangle. Cytokeratin staining of trophoblast cells, which appear in black after

NBT and BCIP staining and counterstaining with PAS and hematoxylin, 40 x magnification. The lower number of trophoblast cells in anti-asialo GM1-treated PE animals is apparent. **A+B:** n=8 uteroplacental units out of 7 anti-asialo GM1-treated PE rats and n=5 uteroplacental units out of 5 control rabbit serum-treated PE rats. In B, n=42 microscopic fields were counted in total in the anti-asialo GM1 PE group and n=29 in total in the control rabbit serum PE group.

Supplementary Figure S3:



Supplementary Figure S3: Influence of anti-asialo GM1 on endovascular trophoblast cell invasion in preeclamptic rats (PE) on pregnancy day 21

A: Anti-asialo GM1 did not change the mean number of infiltrated spiral artery cross sections per mesometrial triangle in PE rats (33.9 ± 4.0 vs. 37.6 ± 9.3 in the control rabbit serum PE group; $p=0.7$, unpaired t-test, shown mean with SEM).

B: The ratio of infiltrated spiral artery cross sections on all spiral artery cross sections within the mesometrial triangle was also not different in PE rats after anti-asialo GM1 application ($46 \pm 3\%$ vs. $52 \pm 9\%$ in the control rabbit serum PE group; $p=0.6$, unpaired t-test with Welch's correction, shown mean with SEM).

C: Anti-asialo GM1 did not change the extent of endovascular trophoblast cell invasion within the circumference of the spiral artery lumen in PE rats (percentage of vessel lumen; score of 2.0 in $n=271$ vs. 2.0 in $n=188$ in the control rabbit serum PE group; $p=0.4$, Mann Whitney test, shown median with interquartile range).

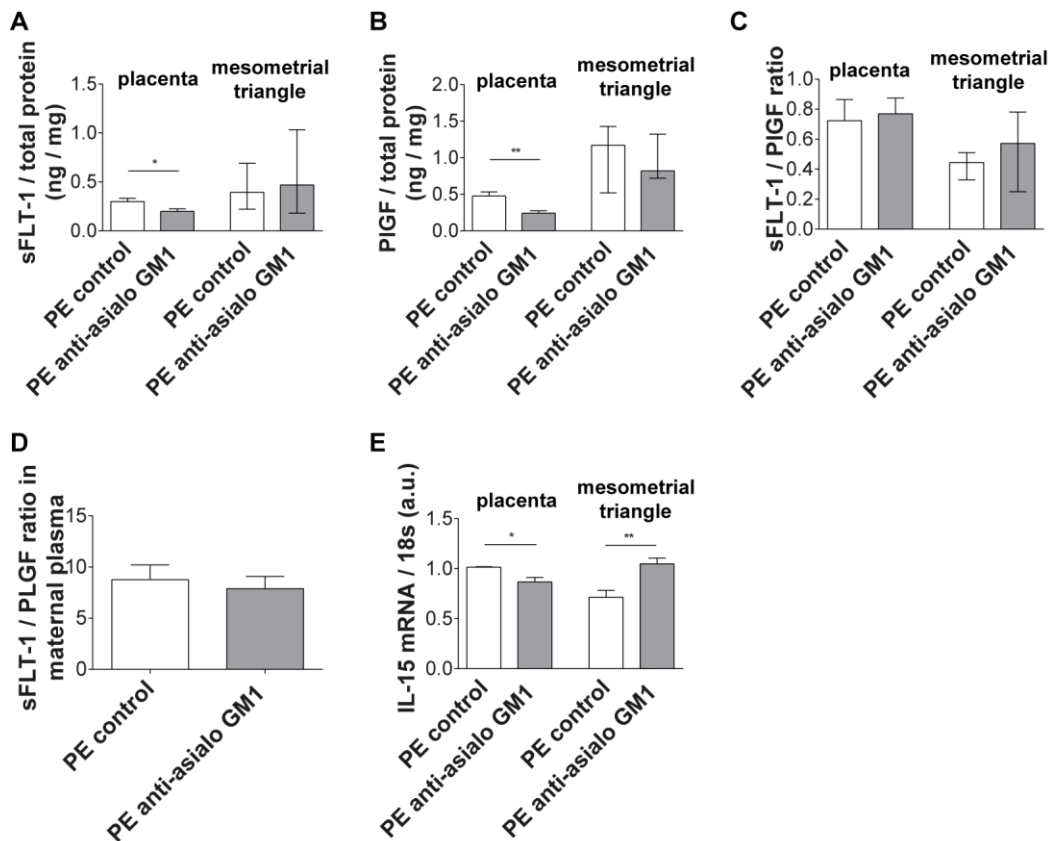
D: The presence of muscle tissue (α -actin) in the wall of trophoblast-invaded spiral artery cross sections was not changed in PE rats after anti-asialo GM1 therapy (score of 3.0 in $n=271$ vs. 3.0 in $n=188$ in the control rabbit serum PE group; $p=0.2$, Mann Whitney test, shown median with interquartile range).

E: Example of an endovascularly invaded spiral artery cross section in a PE rat: On the left, there is a Periodic Acid Schiff staining (PAS) and counterstaining with hematoxylin. It stains fibrinoid red, an extracellular matrix typically secreted by endovascular trophoblast cells. Next to it, there is a cytokeratin staining of trophoblast cells, which appear in black after nitro-blue tetrazolium chloride (NBT) and 5-bromo-4-chloro-3'-indolylphosphate p-toluidine

salt (BCIP) staining and counterstaining with PAS and hematoxylin. The third picture is an α -actin staining of smooth muscle cells, which appear in brown after diaminobenzidine staining and counterstaining with PAS and hematoxylin. On the right, there is a CD31 staining of endothelial cells (again NBT and BCIP staining and counterstaining with PAS and hematoxylin). The arrows highlight the right area of the spiral artery cross section, which is endovascularly invaded by trophoblast cells. In the same area, there is an absence of smooth muscle cells and an accumulation of fibrinoid, which is all together interpreted as remodeling of the artery in this area; all pictures 10 x magnification.

A-D: n=8 uteroplacental units out of 7 anti-asialo GM1-treated PE rats and n=5 uteroplacental units out of 5 control rabbit serum-treated PE rats. In C+D, n=271 spiral artery cross sections were counted in total in the anti-asialo GM1 PE group and n=188 in total in the control rabbit serum PE group.

Supplementary Figure S4:



Supplementary Figure S4: Influence of anti-asialo GM1 on angiogenic profile and interleukin 15 in preeclamptic rats (PE) on pregnancy day 21

A: The soluble fms-like tyrosine kinase 1 (sFLT-1) protein concentration in PE placenta was decreased after anti-asialo GM1 (0.2 ± 0.03 ng/mg total protein vs. 0.3 ± 0.03 ng/mg total protein in the control rabbit serum PE group; $p=0.03$, unpaired t-test, shown mean with SEM); $n=8$ out of 7 anti-asialo GM1-treated PE rats and $n=7$ out of 5 control rabbit serum-treated PE rats, measured by ELISA. The sFLT-1 protein concentration was not different in PE mesometrial triangle (0.5 ng/mg total protein vs. 0.4 ng/mg total protein in the control rabbit serum PE group; $p=0.8$, Mann Whitney test, shown median with interquartile range); $n=3$ out of 3 anti-asialo GM1-treated PE rats and $n=5$ out of 4 control rabbit serum-treated PE rats, measured by ELISA.

B: The placental like growth factor (PIGF) protein concentration in PE placenta was decreased after anti-asialo GM1 (0.2 ± 0.03 ng/mg total protein vs. 0.5 ± 0.06 ng/mg total protein in the control rabbit serum PE group; $p=0.004$, unpaired t-test, shown mean with SEM); $n=7$ out of 6 anti-asialo GM1-treated PE rats and $n=7$ out of 5 control rabbit serum-treated PE rats, measured by ELISA. The PIGF protein concentration was not different in PE mesometrial triangle (0.8 ng/mg total protein vs. 1.2 ng/mg total protein in the control rabbit serum PE group; $p=1.0$, Mann Whitney test, shown median with interquartile range); $n=3$ out of 3 anti-asialo GM1-treated PE rats and $n=5$ out of 4 control rabbit serum-treated PE rats, measured by ELISA.

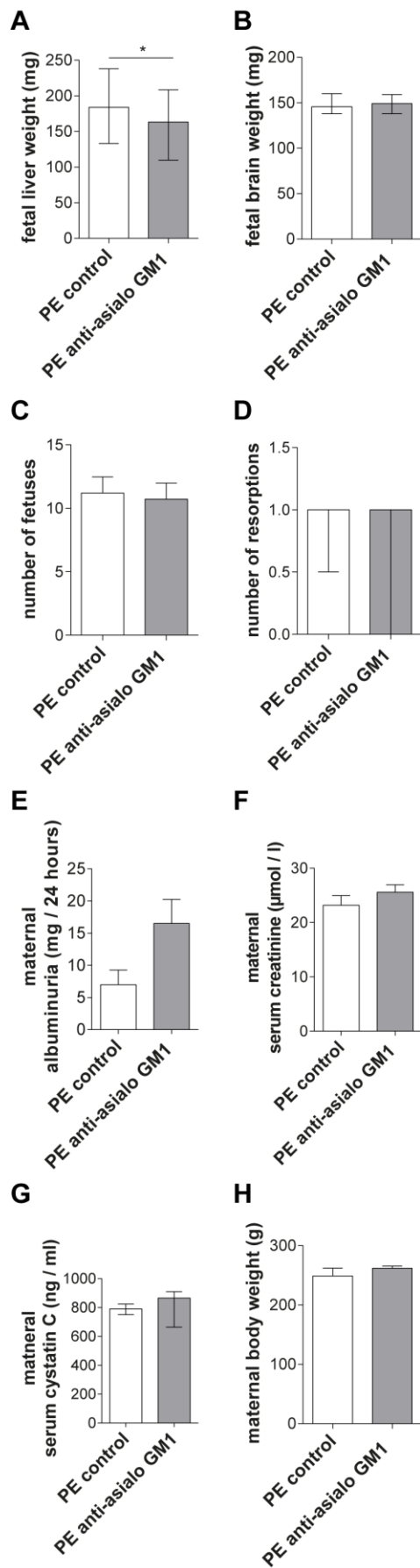
C: There was no difference in the sFLT-1/PLGF ratio in PE placenta (0.8 ± 0.1 vs. 0.7 ± 0.1 in the control rabbit serum PE rats; $p=0.6$, unpaired t-test, shown mean with SEM; $n=7$ out of 6 anti-asialo GM1-treated PE rats and $n=7$ out of 5 control rabbit serum-treated PE rats) or PE mesometrial triangle (0.6 vs. 0.4 in the control rabbit serum PE rats; $p=0.6$, Mann

Whitney test, shown median with interquartile range; n=3 out of 3 anti-asialo GM1-treated PE rats and n=5 out of 4 control rabbit serum-treated PE rats) after anti-asialo GM1 treatment (single values from Supplementary Figures S4A + B).

D: There was no difference in the sFLT-1/PLGF ratio in maternal plasma after anti-asialo GM1 application in PE rats (7.9 ± 1.2 vs. 8.8 ± 1.5 in the control rabbit serum PE group; $p=0.6$, unpaired t-test, shown mean with SEM); measured by ELISA; n=7 rats in the anti-asialo GM1 PE group and n=5 in the control rabbit serum PE group.

E: In the placenta of anti-asialo GM1-treated PE rats, there was a downregulation of interleukin 15 (IL-15) gene expression by 14% ($p=0.03$, unpaired t-test with Welch's correction, shown mean with SEM). In mesometrial triangle, however, anti-asialo GM1 application increased IL-15 expression by 47% ($p=0.006$, unpaired t-test, shown mean with SEM); n=5 per organ per group, measured by quantitative real-time reverse transcription polymerase chain reaction (qRT-PCR).

Supplementary Figure S5:



Supplementary Figure S5: Influence of anti-asialo GM1 on fetal outcome and maternal signs in preeclamptic rats (PE) on pregnancy day 21

A: Fetal liver weight was decreased after treatment with anti-asialo GM1 in PE rats (163.3 mg vs. 183.8 mg in the control rabbit serum PE group; $p=0.03$, Mann Whitney test, shown median with interquartile range); $n=73$ fetuses out of $n=7$ anti-asialo GM1-treated PE mother rats and $n=55$ fetuses out of $n=5$ normal rabbit serum-treated PE mother rats.

B: There was no difference in fetal brain weight between both PE groups after anti-asialo GM1 therapy (149.2 mg vs. 145.6 mg in the control rabbit serum PE group; $p=0.9$, Mann Whitney test, shown median with interquartile range); $n=72$ fetuses out of $n=7$ anti-asialo GM1-treated PE mother rats and $n=55$ fetuses out of $n=5$ normal rabbit serum-treated PE mother rats.

C: Treatment with anti-asialo GM1 did not change mean number of fetuses per PE rat (10.7 ± 1.3 vs. 11.2 ± 1.3 in the control rabbit serum PE group; $p=0.8$, unpaired t-test, shown mean with SEM); $n=7$ mother rats in the anti-asialo GM1 PE group and $n=5$ mother rats in the control rabbit serum PE group.

D: Number of resorptions per PE rat was not different between the two groups (1.0 vs. 1.0 in the control rabbit serum group; $p=0.6$, Mann Whitney test, shown median with interquartile range); $n=7$ mother rats in the anti-asialo GM1 PE group and $n=5$ mother rats in the control rabbit serum PE group.

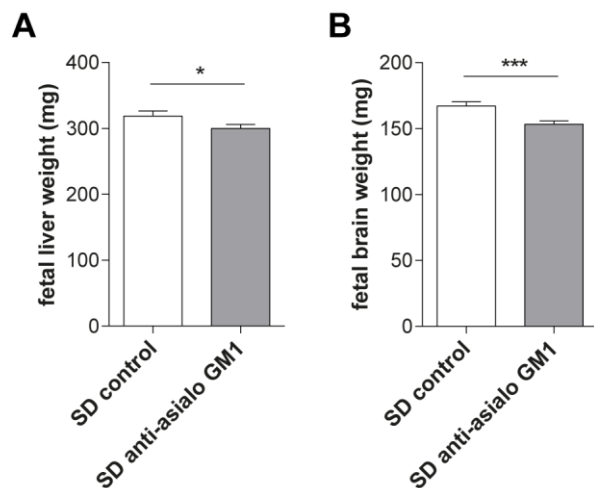
E: Mean 24 hours albuminuria on pregnancy day 18 and 19 was not different after anti-asialo GM1 treatment in PE rats (16.5 ± 3.7 mg vs. 7.0 ± 2.3 mg in the control rabbit serum PE group; $p=0.1$, unpaired t-test, shown mean with SEM); $n=7$ PE mother rats in the anti-asialo GM1 group and $n=5$ PE mother rats in the control rabbit serum group;

F: Serum creatinine after anti-asialo GM1 treatment displayed no difference between both PE groups (25.6 ± 1.4 $\mu\text{mol/l}$ vs. 23.2 ± 1.7 $\mu\text{mol/l}$ in the control rabbit serum PE group; $p=0.3$, unpaired t-test, shown mean with SEM); $n=7$ PE mother rats in the anti-asialo GM1 group and $n=5$ PE mother rats in the control rabbit serum group.

G: Anti-asialo GM1 application did not change serum cystatin C in PE rats (865.9 ng/ml vs. 789.8 ng/ml in the control rabbit serum PE group; $p=0.7$, Mann Whitney test, shown median with interquartile range); $n=7$ PE mother rats in the anti-asialo GM1 group and $n=4$ PE mother rats in the control rabbit serum group.

H: Mean maternal body weight at the end of pregnancy was not different after anti-asialo GM1 treatment in PE rats (262 ± 4 g vs. 249 ± 13 g in the control rabbit serum PE group; $p=0.4$, unpaired t-test with Welch's correction, shown mean with SEM); $n=7$ PE mother rats in the anti-asialo GM1 group and $n=5$ PE mother rats in the control rabbit serum group.

Supplementary Figure S6:



Supplementary Figure S6: Influence of anti-asialo GM1 in wild type Sprague-Dawley rats (SD) on pregnancy day 21

A: Anti-asialo GM1 decreased fetal liver weight in SD rats (299.8 ± 6.0 mg vs. 318.7 ± 7.5 mg in the control rabbit serum SD group; $p=0.0498$, unpaired t-test, shown mean with SEM).

B: Fetal brain weight was decreased after treatment with anti-asialo GM1 in SD rats (153.3 ± 2.4 mg vs. 167.1 ± 3.1 mg in the control rabbit serum SD group; $p=0.0007$, unpaired t-test, shown mean with SEM).

A+B: $n=50$ fetuses out of $n=6$ anti-asialo GM1-treated SD mother rats and $n=46$ fetuses out of $n=6$ normal rabbit serum-treated SD mother rats.